



142  
676  
THS



2310

**MSU is an Affirmative Action/Equal Opportunity Employer**

**PLACE IN RETURN BOX** to remove this checkout from your record.  
**TO AVOID FINES** return on or before date due.  
**MAY BE RECALLED** with earlier due date if requested.

DATE DUE	DATE DUE	DATE DUE

**DIFFERENTIATION OF BULLET TYPE BASED ON ANALYSIS OF GUNSHOT  
RESIDUE USING INDUCTIVELY COUPLED PLASMA MASS SPECTROMETRY**

**By**

**Ruth Norma Udey**

**A THESIS**

**Submitted to  
Michigan State University  
in partial fulfillment of the requirements  
for the degree of**

**MASTER OF SCIENCE**

**Forensic Science**

**2010**



## ABSTRACT

### DIFFERENTIATION OF BULLET TYPE BASED ON ANALYSIS OF GUNSHOT RESIDUE USING INDUCTIVELY COUPLED PLASMA MASS SPECTROMETRY

By

Ruth Norma Udey

Porcine tissue samples shot with two different types of bullets, jacketed and non-jacketed, were collected in the fresh state and throughout moderate decomposition. Wound samples were microwave digested and analyzed using inductively coupled plasma mass spectrometry (ICP-MS) to detect all elements present in gunshot residue (GSR). Elements detected included antimony (Sb), barium (Ba), and lead (Pb), which are considered characteristic of GSR, as well as iron (Fe) and copper (Cu). These five elements were used to differentiate shot tissue and unshot tissue, as well as tissue shot by the two different bullet types, in both the fresh state and throughout moderate decomposition. The concentrations of Cu, Sb, and Pb were able to distinguish between the two bullet types in fresh tissue samples at the 95% confidence level. Copper and Pb were able to differentiate the bullet types throughout moderate decomposition at the 99% confidence level. The source of these distinguishing elements is likely the different bullets. A sampling study carried out on a fresh non-jacketed bullet wound determined that the optimal sampling position to detect all elements considered characteristic of GSR using ICP-MS is directly adjacent to the wound and as far out as two centimeters from the entrance wound in any direction.

## ACKNOWLEDGEMENTS

I would like to thank the many people who assisted and supported me throughout this project. Dr. Ruth Smith was my advisor and was always quick with suggestions and encouragement. Dr. Brian Hunter had great ideas for the project, taught me about pathology, and sat on my committee. Dr. Steve Dow also took time out of his schedule and sat on my committee. Al Snedegar and Kevin Turner from the MSU Swine Facility provided the pigs and helped me transport them. A local certified firearms instructor shot the pigs for me and taught me about ammunition. Matt Parsons assisted with the ICP-MS analyses, and Ron Crichton provided useful input about results interpretation.

I also need to thank the other students in the Forensic Chemistry program, including those who started out when I did and have already graduated as well as current group members. Thanks to Sarah Meisinger, Lucas Marshall, Lisa LaGoo, Jamie Baernkopf, Patty Giebink, Melissa Bodnar, Christy Hay, John McIlroy, Tiffany Van de Mark, Seth Hogg, Kari Anderson, Kaitlin Prather, and Monica Bugeja for talking through problems with me, giving me suggestions, and being such great friends.

Finally, I would like to thank my parents, Dana and Joyce, my sister and her husband, Amanda and Jonathan, and all of my family members for being constant sources of encouragement and perspective. I am truly blessed to have you in my life.

## TABLE OF CONTENTS

<b>List of Tables .....</b>	<b>vi</b>
<b>List of Figures.....</b>	<b>vii</b>
<b>Chapter 1: Introduction .....</b>	<b>1</b>
1.1 Case Study.....	1
1.2 Ammunition .....	2
1.3 Current Forensic Methods for Gunshot Residue Detection .....	5
1.4 Gunshot Residue Detection Using ICP-MS.....	7
1.5 Research Objectives.....	9
1.6 References.....	11
<b>Chapter 2: Theory.....</b>	<b>13</b>
2.1 Histology .....	13
2.2 Microwave Digestion of Porcine Tissue.....	14
2.3 Inductively Coupled Plasma Mass Spectrometry .....	15
2.4 Statistical Procedures .....	19
2.4.1 Analysis of Variance.....	19
2.4.2 Principal Components Analysis.....	24
2.5 References.....	28
<b>Chapter 3: Materials and Methods .....</b>	<b>29</b>
3.1 Experimental Design and Sample Collection .....	29
3.1.1 Fresh Tissue Studies.....	29
3.1.2 Sampling Study .....	30
3.1.3 Decomposition Study .....	32
3.2 Histology .....	32
3.3 Microwave Digestion of Porcine Tissue.....	33
3.4 ICP-MS Analysis of Fresh Tissue Samples .....	34
3.5 Statistical Treatment of Fresh Tissue Data .....	36
3.6 ICP-MS Quantitation of Fresh and Decomposed Tissue Samples .....	37
3.7 Principal Components Analysis of Decomposition Study Data .....	39
3.8 References.....	41
<b>Chapter 4: Results and Discussion .....</b>	<b>42</b>
4.1 Introduction.....	42
4.2 Fresh Tissue Sample Observations and Histology Results.....	42
4.3 Selection of Elements to Discriminate Bullet Types .....	44
4.4 Quantitation of Elements in Fresh Tissue Samples .....	48
4.5 Sampling Study Tissue Observations .....	52
4.6 Quantitation of Elements in Sampling Study Tissue Samples.....	53
4.7 Decomposition Study Observations and Histology Results .....	58



4.8 Quantitation of Elements in Tissue Samples Throughout	
Moderate Decomposition.....	63
4.9 Principal Components Analysis of Decomposition Study Data .....	68
4.10 References .....	73
<b>Chapter 5: Conclusions and Future Directions.....</b>	<b>74</b>
5.1 Conclusions.....	74
5.2 Future Directions.....	78
<b>Appendix .....</b>	<b>81</b>

## LIST OF TABLES

Table 2.1 – Summary of sum of squares and degrees of freedom calculations .....	21
Table 3.1 – ICP-MS parameters for full mass scan and selected ion monitoring (SIM) analyses .....	35
Table 4.1 – Limits of quantitation (LOQs) and SRM recovery results for elements of interest in the fresh tissue study .....	49
Table 4.2 – Limits of quantitation (LOQs) and SRM recovery results for elements of interest in the sampling study.....	54
Table 4.3 – Summary of distances that elements of interest in shot tissue samples were detected at higher levels than procedural blank and control tissue samples..	57
Table 4.4 – Limits of quantitation (LOQs) and SRM recovery results for elements of interest in the decomposition study.....	63
Table 4.5 – Element concentration ranges throughout moderate decomposition in each tissue sample type .....	64

## LIST OF FIGURES

Figure 1.1 – Jacketed (left) and non-jacketed (right) ammunition cartridges.....	3
Figure 2.1 – Schematic of an ICP-MS system .....	16
Figure 2.2 – Example results of PCA visualized as scores and loadings plots.....	27
Figure 3.1 – Diagram of wound where tissue samples were excised for analysis.....	31
Figure 4.1 – Gunshot wounds in fresh porcine tissue from (a) jacketed bullets and (b) non-jacketed bullets, along with corresponding micrographs of H & E stained histology results (c and d, respectively). Refractive particles of unburned gunpowder are circled in the jacketed bullet wound histology slide (c), and dark granules of burned gunpowder are circled on the non-jacketed bullet wound histology slide (d).....	43
Figure 4.2 – Mean concentrations of elements of interest in the first fresh tissue study (procedural blank n = 3, control n = 3, jacketed n = 9, and non-jacketed n = 9). The error bars represent one standard deviation. Significant difference between element concentrations at 99% confidence level ( $p \leq 0.01$ ) are indicated by ** .....	47
Figure 4.3 – Mean concentrations of elements of interest quantified in fresh tissue samples (procedural blank n = 6, control n = 1, jacketed n = 5, and non-jacketed n = 5). The error bars represent one standard deviation. Significant difference between element concentrations at 95% confidence level ( $p \leq 0.05$ ) are indicated by * and significant difference between element concentrations at 99% confidence level ( $p \leq 0.01$ ) are indicated by ** .....	51
Figure 4.4 – Sampling study wound (a) before tissue sections were removed and (b) after tissue samples had been removed for analysis. The four directions that the tissue was sampled are indicated with arrows.....	53
Figure 4.5 – Concentrations of (a) Fe, (b) Sb, (c) Ba, and (d) Pb quantitated in the sampling study samples (procedural blank n = 3, control n = 3, and non-jacketed n = 1). Error bars are one standard deviation. In the 3:00 direction data, “6 cm/edge” indicates that the wound edge was at 6 cm .....	55
Figure 4.6 – Jacketed bullet wounds on days 0, 29, and 49 during the decomposition study. Corresponding micrographs of H & E stained histology results are shown below the wounds, with particles consistent with GSR circled.....	60



Figure 4.7 – Non-jacketed bullet wounds on days 0, 29, and 49 during the decomposition study. Corresponding micrographs of H & E stained histology results are shown below the wounds, with particles consistent with GSR circled.....	61
Figure 4.8 – Control (stab) wounds on days 0, 29, and 49 during the decomposition study. Corresponding micrographs of H & E stained histology results did not show any particles consistent with GSR, as expected .....	62
Figure 4.9 – Mean concentrations of elements of interest quantified in samples collected throughout moderate decomposition (procedural blank n = 5, control (fresh) n = 3, control (decomposed) n = 6, jacketed and non-jacketed n = 6). The error bars represent one standard deviation. Significant difference between element concentrations at 99% confidence level ( $p \leq 0.01$ ) are indicated by ** .....	66
Figure 4.10 – PCA scores plot displaying clustering of chemically similar samples.....	69
Figure 4.11 – PCA loadings plot showing the elements responsible for the sample positions displayed in the corresponding scores plot.....	69

## **CHAPTER 1: INTRODUCTION**

### **1.1 Case Study**

Conventionally, gunshot wound determinations are made using gross injury examination at autopsy by visualization of gunshot residue (GSR). However, interpretation of gunshot wounds can be difficult even when the deceased individual is well preserved, since the characteristics of gunshot wounds vary greatly based on the type of firearm and ammunition used, range of fire, and the location of the wound on the body. When post-mortem factors such as decomposition, burial, and insect activity are present, the identification of a gunshot wound becomes even more challenging, as illustrated by the following case presented to a local forensic pathologist in 2004.<sup>1</sup>

The decedent was a 25 year old white male whose body was found buried in a remote area one year after he went missing. His soft tissues had a soapy, mushy quality consistent with adipocere. Police investigation and the shirt recovered with the victim indicated that he had been shot in the torso, however, the malleable nature of the tissues made identification of the entrance wounds only possible through palpation. The poor preservation of the tissue also prevented detection of GSR by gross or histologic examination.

Clinical scenarios such as this demonstrate the need for ways to increase confidence in GSR determination by using chemical means of detection that are not affected by decomposition. In order to design suitable chemical detection methods, the content of GSR must first be understood.

## 1.2 Ammunition

Small-arms ammunition cartridges consist of a cartridge case, a primer, propellant (gunpowder), and a bullet [Figure 1.1]. When a weapon is fired, the firing pin strikes the center of the primer cup, compressing the primer and causing it to explode. Small flash holes allow the flame to pass into the cartridge case, igniting the propellant. The combustion of the propellant leads to gas formation and the increased pressure forces the bullet down the gun barrel. The heated primer also partially vaporizes and is released from the gun along with the propellant combustion products and unburned propellant. This combination of materials is known as GSR.<sup>2</sup> While some research has analyzed the organic compounds in the propellant,<sup>3</sup> the chemical detection of GSR in forensic labs focuses on the metals in the primer (antimony (Sb), barium (Ba), and lead (Pb)). However, vaporized metals from the cartridge case, bullet, and gun barrel that were present in the hot gas cloud emitted during discharge could also be present in GSR.<sup>2</sup>



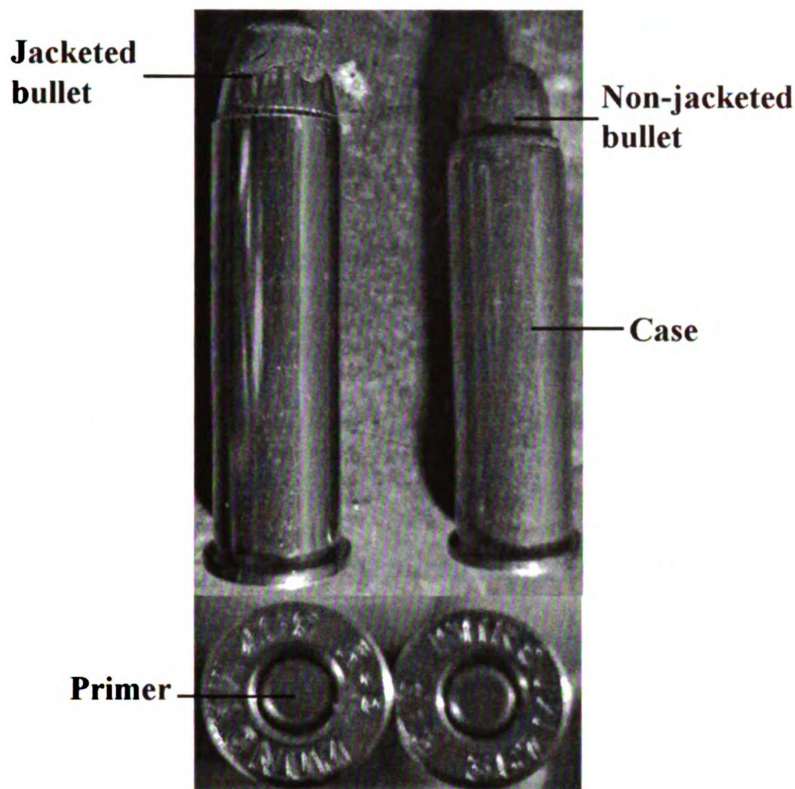


Figure 1.1 – Jacketed (left) and non-jacketed (right) ammunition cartridges.

Cartridge cases are usually made of brass, with a composition of 70% copper and 30% zinc, but some are plated with nickel or made of steel or aluminum. The main functions of the cartridge case are to hold the propellant and to expand and seal the gun chamber so that all gases escape in the forward direction when the cartridge is fired.<sup>2</sup>

The primer is located in the primer cup in the base of the cartridge and is used to initiate ignition of the propellant. The primer is composed of an explosive, an oxidizer, and a fuel, and it is stable but explosive upon impact. The most common primer compounds are lead styphnate (explosive), barium nitrate (oxidizer), and antimony sulfide (fuel). The detection of these compounds is the basis for tests to determine whether an individual has fired a firearm. Some ammunition manufacturers have

removed the lead styphnate from the primer composition due to environmental concerns, while other manufacturers use only lead styphnate or only lead styphnate and barium nitrate. However, these ammunition types are uncommon as they are designed for specific purposes or specific firearms.<sup>2</sup>

The propellant is commonly smokeless gunpowder composed of nitrocellulose (single-base), nitrocellulose and nitroglycerine (double-base), or nitrocellulose, nitroglycerine, and nitroguanidine (triple-base). The individual powder grains can be shaped as disks, flakes, or cylinders, depending on the desired burning rate of the powder. The propellant itself is relatively stable against ignition, hence the need for the primer to initiate the burning of the propellant. It is the rapid burning of the propellant and release of gaseous products that pushes the bullet out of the firearm.<sup>2</sup>

The bullet is the part of the cartridge that leaves the barrel of the firearm when it is discharged. Bullets fall into two composition categories: lead bullets and metal-jacketed bullets. Lead bullets are made principally of lead with antimony and/or tin added to increase hardness. Metal jacketed bullets have a lead or steel core that is covered by an outside jacket composed of copper with zinc, steel, copper with nickel, or aluminum. The bullets may be either full-jacketed or partially-jacketed, with the bullet core totally covered in full-jacketed ammunition and the core partially exposed in partially-jacketed ammunition.<sup>2</sup>

### **1.3 Current Forensic Methods for Gunshot Residue Detection**

Coroners, medical examiners, and forensic pathologists routinely use histology procedures to determine the presence of GSR in tissue sections from a suspected gunshot wound. Tissue sections cut from samples taken adjacent to the wound are stained using hematoxylin and eosin (H & E) and examined using light microscopy. Particles of burned gunpowder appear as fine, dark granules, and larger pieces of unburned gunpowder appear lighter in color as they refract the incident light. However, as the stain does not react with the GSR particles themselves, only the tissue, any particles observed in the tissue sections cannot be definitively identified as GSR. This becomes a problem when there is debris present on the body, resulting from burial for example, as soil and sand particles can appear similar to burned and unburned gunpowder during both gross and histological examination. Tissue also becomes more difficult to section as decomposition progresses. These difficulties would be overcome by a chemical detection method suitable for use on tissue at any stage of decomposition.

Gunshot residue has been detected in fresh animal hide using staining and visual examination techniques.<sup>4, 5</sup> Shot human tissue samples have also been analyzed for GSR using staining and X-ray microfluorescence, but these studies focused on fresh, rather than decomposing, tissue and did not use the instrumental methods described below.<sup>6, 7</sup>

Crime laboratories today use scanning electron microscopy with energy dispersive X-ray spectroscopy (SEM/EDS) to identify GSR on possible assailants or victims' skin or clothing to help confirm a wound as a gunshot wound. Particles suspected to contain GSR are collected by dabbing an adhesive tab mounted on an aluminum stub across a surface. Analysis using SEM/EDS provides both particle morphology and elemental



composition which are used to definitively identify GSR particles.<sup>2</sup> Wolten *et al.* described four elemental combinations that were observed in GSR particles and were therefore regarded as characteristic of GSR.<sup>8</sup> The most prominent of these combinations was Sb, Ba, and Pb, which come from ammunition primers and bullets.<sup>9</sup> However, SEM/EDS is limited by the ability to locate GSR particles on the adhesive tab, which becomes difficult if the particles are embedded in the adhesive or are obscured by other debris from the sample.<sup>10, 11</sup> While automated software programs are available, the analysis can still be time-consuming, taking up to several hours per cm<sup>2</sup> of sample.<sup>12</sup> Also, it becomes difficult to effectively collect particles from decomposing tissue using the adhesive stubs, especially when outdoors, as the tissue becomes oily.<sup>13</sup>

Differentiation of jacketed and non-jacketed bullets based on elements present in GSR was demonstrated by Wunnapuk *et al.* in 2007.<sup>14</sup> Fresh wounds in human tissue were used in the study and were analyzed using inductively coupled plasma atomic emission spectroscopy (ICP-AES). Wounds were digested using nitric acid and heating at 100 °C for two hours. After filtering and dilution, the tissue digests were analyzed using ICP-AES in a semi-quantitative manner. Lead and antimony were significantly more concentrated in non-jacketed bullet wounds compared to jacketed bullet wounds, as was barium although the difference in concentration was not significant. Copper and iron were more concentrated in the jacketed bullet wounds compared to non-jacketed bullet wounds, though the differences were not significant. The concentration of zinc was similar for both bullet types. However, not all of the elements were useful for

differentiating between control tissue and tissue shot with both bullet types. The study concluded that a high content of iron and zinc was deposited in wounds shot with jacketed bullets, and a high concentration of lead was deposited as a result of a non-jacketed bullet wound. These elements were likely due to the bullet and casing compositions.<sup>14</sup> While this study demonstrated the analysis of tissue surrounding a gunshot wound, it is likely that the digestion procedure was not sufficient to completely digest the tissue and release all of the elements of interest into solution. Also, the study focused on fresh tissue samples and did not take the effects of decomposition into account. In addition, the analysis was not rigorously quantitative, so element concentrations are not expected to be as accurate as they could be. Detection limits for ICP-AES analysis were not reported in this particular study, however, it is well known that other techniques, such as inductively coupled plasma mass spectrometry, have detection limits between one and three orders of magnitude lower than ICP-AES, depending on which elements are being analyzed.<sup>15</sup>

#### **1.4 Gunshot Residue Detection Using ICP-MS**

Inductively coupled plasma mass spectrometry (ICP-MS) has also been used for the determination of Sb, Ba, and Pb in GSR, as well as simulated samples of GSR.<sup>16-18</sup> Analysis using ICP-MS was successful in determining these three elements of interest from extracts of swabs spiked with the three elements,<sup>16</sup> extracts of swabs from shooter's hands,<sup>16, 17</sup> and from digests of shot cotton tissue.<sup>18</sup> Koons described the analysis of standard solutions containing Sb, Ba, and Pb, as well as extract solutions from cotton

swabs either spiked with Sb, Ba, and Pb or taken from shooters' hands, using ICP-MS.<sup>16</sup>

Both standard and swab extract solutions showed linear responses over the entire dynamic range of the instrument, from the limit of detection to the maximum detectable signal, indicating that no matrix effects from the cotton swabs were present. The relative standard deviation of replicate measurements was less than 5% for all three elements, demonstrating the high precision of the instrument. The detection limits were determined to be 0.052 µg/L for Sb, 0.020 µg/L for Ba, and 0.014 µg/L for Pb. The limits of detection for the three elements were at least one order of magnitude less than levels typically observed in GSR (40-500 ng), and were lower than corresponding detection limits using graphite furnace atomic absorption spectroscopy and ICP-AES. The ability to detect Sb, Ba, and Pb in extracts of swabs from shooters' hands by ICP-MS was also comparable to the two other analytical techniques.<sup>16</sup>

Santos *et al.* used a target of cotton tissue, and the resulting GSR deposition pattern was analyzed by ICP-MS to estimate firing distance.<sup>18</sup> Samples of the cotton tissue were removed from different distances around the entrance wound and digested with nitric acid prior to analysis. The detection and quantitation of Sb, Ba, and Pb deposited on the cotton tissue was possible at firing distances ranging from 20 to 80 cm in four radial positions ranging from 1.5 to 5.5 cm from the entrance hole. The best radial position for sample collection was determined to be between 3.5 and 4.5 cm from the entrance hole in order to most accurately determine the firing distance.<sup>18</sup> However, these results are only valid for the specific gun and ammunition used and cannot be applied to other firearms.

The use of ICP-MS to analyze digested bullet shavings to differentiate bullets according to elemental composition has also been described, but the resulting GSR was not analyzed to determine if the residue could be used to differentiate the bullets as well.<sup>19-21</sup>

The studies outlined thus far have focused on the detection of GSR deposited on the hands of a shooter or other surfaces using ICP-MS. Until very recently the analysis of GSR tattooed into tissue surrounding a gunshot wound had not been attempted using ICP-MS. LaGoo *et al.* demonstrated the ability of ICP-MS to detect Sb, Ba, and Pb in shot porcine tissue throughout decomposition.<sup>13</sup> Analysis of microwave digested wound tissue allowed the detection of GSR at all stages during decomposition in both late summer and winter months. Wounds were also analyzed using SEM/EDS for comparison, and GSR was only identified on the first day of the study, after which rain washed away surface particles and prevented collection using adhesive tabs. Detection of GSR by ICP-MS was shown to be unaffected by environmental conditions, and it was also shown that concentrations of GSR detected in tissue depended more on the stage of decomposition rather than the time since death.<sup>13</sup> While the study showed success in detecting Sb, Ba, and Pb, there was no attempt to detect any other elements that may be present in GSR.

### **1.5 Research Objectives**

Gunshot wounds in decomposing tissue are difficult to identify, making chemical means of detection necessary. While work has been done to detect Sb, Ba, and Pb in

tissue using ICP-MS, the potential to detect additional elements that may provide further information about the bullet or gun used to make the wound has not been investigated.

Therefore, the goals of this research were:

- To identify additional elements characteristic of GSR in order to increase confidence in gunshot wound determination using ICP-MS.
- To differentiate two bullet types, jacketed and non-jacketed, using their characteristic element profiles.
- To assess the effects of moderate decomposition on the ability to detect GSR and differentiate bullet types.

The results of this research will benefit law enforcement agencies as well as coroners, medical examiners, and forensic pathologists. Law enforcement agencies may use the method to determine the type of bullet used, which can link a weapon and/or suspect to a crime scene. Coroners, medical examiners, and forensic pathologists could also use the method to assist in gunshot wound identification and cause of death determination, even in corpses in a moderate state of decomposition.

## **1.6 References**

1. MacAulay LE, Barr DG, Strongman DB. Effects of decomposition on gunshot wound characteristics: under moderate temperatures with insect activity. *J Forensic Sci* 2009;54:443-7.
2. Di Maio VJM. Gunshot wounds: practical aspects of firearms, ballistics, and forensic techniques. 2nd ed. Boca Raton: CRC Press, 1999.
3. Scherperel G. Electrospray ionization mass spectrometry for the detection and characterization of smokeless powders [thesis]. East Lansing (MI): Michigan State University, 2007.
4. Brown H, Cauch DM, Holden JL, Wrobel H, Cordner S. Image analysis of gunshot residue on entry wounds - I - the technique and preliminary study. *Forensic Sci Int* 1999;100:163-77.
5. Brown H, Cauchi DM, Holden JL, Allen FCL, Cordner S, Thatcher P. Image analysis of gunshot residue on entry wounds - II - a statistical estimation of firing range. *Forensic Sci Int* 1999;100:179-86.
6. Glattstein B, Zeichner A, Vinokurov A, Levin N, Kugel C, Hiss J. Improved method for shooting distance estimation. Part III. Bullet holes in cadavers. *J Forensic Sci* 2000;45:1243-9.
7. Brazeau J, Wong RK. Analysis of gunshot residues on human tissues and clothing by X-ray microfluorescence. *J Forensic Sci* 1997;42:424-8.
8. Wolten GM, Nesbitt RS, Calloway AR, Loper GL, Jones PF. Particle analysis for the detection of gunshot residue. 1. Scanning electron microscopy energy dispersive X-ray characterization of hand deposits from firing. *J Forensic Sci* 1979;24:409-22.
9. Stone IC, Di Maio VJM, Petty CS. Gunshot wounds - visual and analytical procedures. *J Forensic Sci* 1978;23:361-7.
10. Matricardi VR, Kilty JW. Detection of gunshot residue particles from hands of a shooter. *J Forensic Sci* 1977;22:725-38.
11. Romolo FS, Margot P. Identification of gunshot residue: a critical review. *Forensic Sci Int* 2001;119:195-211.
12. Zeichner A. Recent developments in methods of chemical analysis in investigations of firearm-related events. *Anal Bioanal Chem* 2003;376:1178-91.
13. LaGoo L, Schaeffer LS, Szymanski DW, Waddell Smith, R. Detection of gunshot residue in blowfly larvae and decomposing porcine tissue using inductively coupled



plasma mass spectrometry (ICP-MS). *J Forensic Sci* 2010;55:624-32.

14. Wunnapuk K, Durongkadech P, Minami T, Ruangyuttikarn W, Tohno S, Vichairat K, Azuma C, Sribanditmongkol P, Tohno Y. Differences in the element contents between gunshot entry wounds with full-jacketed bullet and lead bullet. *Biol Trace Elem Res* 2007;120:74-81.
15. Skoog DA, Holler FJ, Nieman TA. *Principles of instrumental analysis*. 5th ed. Toronto: Thomson Learning, 1998.
16. Koons RD. Analysis of gunshot primer residue collection swabs by inductively coupled plasma-mass spectrometry. *J Forensic Sci* 1998;43:748-54.
17. Sarkis JES, Neto ON, Viebig S, Durrant SF. Measurements of gunshot residues by sector field inductively coupled plasma mass spectrometry - further studies with pistols. *Forensic Sci Int* 2007;172:63-6.
18. Santos A, Magalhaes T, Vieira DN, Almeida AA, Sousa AV. Firing distance estimation through the analysis of the gunshot residue deposit pattern around the bullet entrance hole by inductively coupled plasma-mass spectrometry - an experimental study. *Am J Foren Med Path* 2007;28:24-30.
19. Dufosse T, Touron P. Comparison of bullet alloys by chemical analysis: use of ICP-MS method. *Forensic Sci Int* 1998;91:197-206.
20. Keto RO. Analysis and comparison of bullet leads by inductively-coupled plasma mass spectrometry. *J Forensic Sci* 1999;44:1020-6.
21. Suzuki Y, Marumo Y. Determination of trace impurities in lead shotgun pellets by ICP-MS. *Anal Sci* 1996;12:129-32.

## **CHAPTER 2: THEORY**

### **2.1 Histology**

Histology is the study of tissues and microscopic cellular details by pathologists for a variety of medical diagnostic applications.<sup>1</sup> Staining of thin tissue sections allows visualization of structural details at the cellular level. In order to study pathological material, sections of tissue are stained in such a way as to impart dark color to the nuclei of cells and a lighter, contrasting color to the cytoplasm and extracellular structures. The most common histology staining method used by pathologists is hematoxylin and eosin (H & E) staining.<sup>2</sup> The first part of the stain, hematoxylin, is positively-charged and colors the nuclei of cells blue by binding to negatively-charged nucleic acids in DNA. The eosin counterstain is negatively-charged and colors both intracellular and extracellular proteins pink by binding to positively-charged amino acids, resulting in cell cytoplasm staining.<sup>3</sup> Stained tissue sections are examined using light microscopy to determine any structural irregularities that might give information as to disease or the cause of a wound.<sup>2</sup>

While H & E staining of tissue sections is useful, the stains are not highly selective, and are only designed to aid visualization. Any debris present on the tissue section, such as gunshot residue, may be visible, but the H & E stain is not designed to react with non-biological material. Therefore, histology cannot be used for definitive identification of GSR and hence is very limited for this application.<sup>2</sup>

## **2.2 Microwave Digestion of Porcine Tissue**

Analytical techniques capable of multi-element quantitation require that solid matrices, such as skin tissue, be converted into a liquid prior to analysis. As biological samples contain a mixture of proteins, lipids, and carbohydrates, they are not completely soluble in either aqueous or organic solvents. It is therefore necessary to decompose the biological matrix, which can be achieved using microwave digestion. While there are numerous methods designed to microwave digest biological samples, the majority of sample preparation protocols employ closed systems. Biological samples to be digested are sealed inside vessels containing strong oxidizing agents such as acids and peroxides. Nitric acid is by far the most common digestion agent as it effectively decomposes the organic matrix of the sample and liberates elements into solution as soluble nitrate salts.<sup>4</sup>

The closed microwave digestion vessels are placed in a microwave oven which is very similar to domestic microwave ovens. Microwave irradiation causes polar molecules within a sample to rotate, causing friction with neighboring molecules and releasing heat. As the sample is heated, the pressure inside the sealed vessel increases due to the evaporation of the digestion acids and gases that are evolved during the breakdown of the biological matrix. As pressure within the vessel increases, the boiling point of the digestion reagents also increases, resulting in more efficient breakdown of the sample matrix. This build-up of pressure is closely controlled by monitoring the temperature inside the digestion vessels using a temperature probe. Microwave power is only applied when the temperature reading is below the user specified level, ensuring that the temperature and pressure inside the microwave vessel do not exceed safety limits. The

resulting digest solution is free of solid material and contains all analytes of interest in a soluble form that is compatible with the desired analytical detection method.<sup>4</sup>

Open microwave digestion systems, while devoid of pressure build-up problems, require an effective fume removal system. The continuous removal of vapors decreases the concentration of digestion reagents in the vessel, and hence the digestion efficiency decreases as well. The variable concentration of digestion reagents remaining in the vessel also decreases the precision of replicate digestions in open systems. The danger of sample contamination or loss through the open vessel is undesirable as well. Therefore, the major advantages of a closed microwave digestion system are that high heating efficiency is obtained with a decreased risk of sample loss. The precise monitoring of temperature inside the closed digestion vessels also yields very reproducible digestions.<sup>4</sup>

### **2.3 Inductively Coupled Plasma Mass Spectrometry**

Inductively coupled plasma mass spectrometry (ICP-MS) is one of the most widely used techniques for elemental analysis because of its low detection limits, high degree of selectivity, large linear dynamic range, short analysis times, and good precision and accuracy. The concentrations of numerous elements may be determined simultaneously in a liquid sample using this technique. Elements are ionized using a plasma torch and then separated and detected using a mass spectrometer. The mass spectrometer separates the elements by their mass to charge ( $m/z$ ) ratio and detects the abundance of each element present in the sample. Qualitative, semi-quantitative, and quantitative analyses are all possible with the addition of internal standards and the use of external calibration curves.<sup>5</sup>

A schematic of an ICP-MS instrument is shown in Figure 2.1. The liquid sample solution is introduced into the argon (Ar) plasma torch, and the resulting ions are directed through two nickel-plated cones into the mass spectrometer, where they are separated based on their  $m/z$  ratio by a quadrupole mass analyzer. Although other mass analyzers, such as time of flight or ion trap, may also be used for ion separation, in this research a quadrupole mass analyzer was used. The ions are then detected using a conversion dynode and electron multiplier.<sup>5</sup>

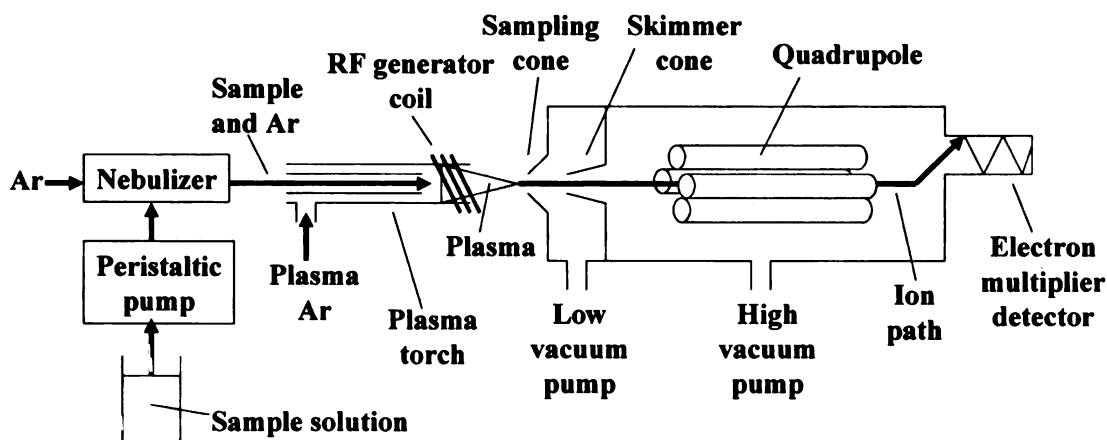


Figure 2.1 – Schematic of an ICP-MS system. .

The ICP torch is composed of three concentric quartz tubes through which streams of Ar flow. The innermost tube contains sample droplets carried toward the plasma by an Ar stream. Argon flowing through the middle tube supports the plasma. The outermost Ar flow cools the induction coil surrounding the torch. The plasma is generated by exposing the flow of Ar gas to Tesla sparks that initiate ionization of the flowing gas. The resulting ions and electrons then interact with the high-frequency

oscillating inductive field created by the RF current generated in a coil wrapped around the torch. The ions and electrons are consequently accelerated, collide with more Ar atoms, and subsequently ionize them. This ionization cascade continues until the ionization process is balanced with the ion-electron recombination process, resulting in the plasma. All of the ion and electron collisions cause heating of the plasma to approximately 10,000 K.<sup>6</sup>

The sample solution is introduced into the plasma torch using a peristaltic pump and nebulizer. A flow of Ar gas through the nebulizer produces a fine aerosol spray of sample that is then carried into the hot plasma. The high temperature of the plasma rapidly desolvates, vaporizes, atomizes, and ionizes the elements in the sample into singly charged positive ions. The ions are then extracted from the plasma using a negative potential and are introduced into the mass spectrometer portion of the instrument through two cooled nickel cones. The sampling and skimmer cones separate differentially pumped regions of an interface which separates the  $10^{-5}$  torr vacuum environment of the mass spectrometer from the plasma torch ion source at atmospheric pressure. Once inside the mass spectrometer, the ion beam is accelerated and focused using an ion lens toward the entrance of the quadrupole mass analyzer.<sup>6</sup>

The quadrupole mass analyzer uses the stability of ion trajectories in oscillating electric fields to separate them according to their  $m/z$  ratio. The analyzer consists of four parallel cylindrical rods. Opposite rods are connected electrically, with one pair connected to the negative terminal of a variable direct current (dc) source and the other pair connected to the positive side. A variable radio-frequency alternating current (ac)

potential is also applied to the pairs of rods. As ions are accelerated into the quadrupole, the ac and dc voltages on the rods are increased simultaneously so that their ratio remains constant. The ions travel in a helical pattern through the quadrupole, and at any given moment, only those ions with a certain  $m/z$  value have stable trajectories and hence reach the detector. All other ions collide with the rods, are neutralized, and are not detected. The quadrupole can be used to scan a range of  $m/z$  values (full mass scan), or can be used to allow only selected masses to reach the detector (selected ion monitoring). The latter, also known as SIM, increases the sensitivity of the instrument as more time is spent monitoring the signals from the ions of interest.<sup>5</sup>

The ions that pass through the quadrupole are detected using a conversion dynode and electron multiplier. The positively charged ions are accelerated toward the conversion dynode using a -15 kV potential. When the ion strikes the conversion dynode, secondary electrons are ejected from the surface. These electrons are accelerated toward the next dynode, which is held at a more positive potential, and when they strike the dynode more secondary electrons are ejected from the surface. This cascade of electron multiplication results in an amplified current that is directly proportional to the number of ions of that specific  $m/z$  ratio that passed through the quadrupole at a given time. It is important to note that the conversion dynode is slightly offset from the exit of the quadrupole to prevent light from the plasma torch from striking the conversion dynode, as that would create secondary electrons as well and cause errors in ion abundance measurement. The output of the detector is a mass spectrum which is a plot of ion abundance versus  $m/z$  ratio. Ion abundance corresponds to the concentration of each

element present in the sample, so that quantification of elements is possible using this technique.<sup>6</sup>

## **2.4 Statistical Procedures**

### *2.4.1 Analysis of Variance*

Analysis of variance (ANOVA) is a powerful statistical procedure that can be used to separate and estimate the different sources of variation in a sample set. It is used when there are more than two means to be compared in an analytical experiment, and thus two possible sources of variation: random error, which is always present, and variation due to a controlled or fixed-effect factor, i.e. an experimental variable that is purposely varied. It is used to separate any variation caused by changing the controlled factor (between-sample variation) from the variation due to random error (within-sample variation), which is useful for testing whether the controlled factor itself leads to a significant difference between the mean values obtained. Analysis of variance can also be used in situations where there are two random sources of variation, such as the random nature of sampling aliquots of a whole specimen for testing, in addition to the ever-present random error in measurement. Since the sampling is done at random, the variation will be random and is termed a random-effect factor. Analysis of variance is still useful for separating and estimating two random sources of variation. Both types of statistical analyses, i.e. where there is one factor, either controlled or random, in addition to the random error in measurement, are known as one-way ANOVA.<sup>7</sup>

In the case of two random factors, one-way ANOVA is used to separate and estimate the different sources of variation: that due to random error, called measurement



variance, and that due to real variations in the sample, called sampling variance, which is a random-effect factor. In this case, the calculated within-sample variance is used to estimate the measurement variance. However, the calculated between-sample variance is no longer an appropriate measure of the sampling variance because the variation between sample means is caused by both measurement variance and sampling variance simultaneously. Therefore, methods to adjust the between-sample variance calculation to more accurately estimate the variation due to sampling variance alone need to be employed.<sup>7, 8</sup>

The magnitudes of the different sources of variation are calculated separately using sum of squares terms in order to test whether the difference between the sample means is too large to be explained by the random error alone [Table 2.1]. In general, a sum of squares term is used to calculate the sum of the differences between each individual measurement and the mean of all measurements. The difference is squared to make all the differences positive, instead of some positive and some negative, so that they can be accurately summed. The within-sample mean square is determined by calculating the difference between the total and between-sample mean squares for simplicity.<sup>7</sup>

Table 2.1 – Summary of sum of squares and degrees of freedom calculations.<sup>7</sup>

Source of Variation	Sum of Squares	Degrees of Freedom
Between-samples	$\sum_i \frac{T_i^2}{n} - \frac{T^2}{N}$	$h - 1$
Within-samples	by subtraction	by subtraction
Total	$\sum_i \sum_j x_{ij}^2 - \frac{T^2}{N}$	$N - 1$

where:  $n$  = number of replicates  
 $h$  = number of samples  
 $N = nh$  = total number of measurements  
 $x_{ij}$  = one measurement  
 $T_i$  = sum of the measurements in the  $i$ th sample  
 $T$  = sum of all the measurements, grand total

The sum of squares terms have different degrees of freedom associated with them, and hence cannot be directly compared. Degrees of freedom is a determination of the number of measurements in a dataset that are free to vary, which is generally all of them minus one. The minus one restriction is necessary when the calculation of an estimate of one statistic (i.e. sum of squares) is based on an estimate of another statistic (i.e. mean). Sum of square terms with different degrees of freedom can be compared based on the mean square term, which is calculated as follows:

$$\text{mean square} = \text{sum of squares/degrees of freedom.}$$

The mean squares are the variances from different sources that are compared to determine if the variance between samples (fixed- or random-effect variance) is

significantly greater than the variance within samples (measurement variance). To do this, the mean square terms are used in an  $F$ -test as follows:

$$F = \text{between-sample mean square} / \text{within-sample mean square}.$$

The resulting value is then compared to a statistical table of critical  $F_{h-1, N-h}$  values at the desired confidence level. If the critical value of  $F$  is larger than the calculated value of  $F$ , the two sources of variance are not significantly different and all variance in the dataset is due to random measurement variance. Conversely, if the calculated  $F$  value is larger than the critical  $F$  value, the two mean square values are significantly different, and there is variance between samples due to either a fixed- or random-effect factor in addition to the random measurement variance.<sup>7</sup>

In the case of a significant random-effect factor (i.e. sampling variance), corrections may be employed to the between-sample mean square calculation to more accurately estimate the magnitude of the sampling variance alone. There are two corrections that can be used as estimators of the sampling variance: the method of moments and the Klotz-Milton-Zacks estimator.<sup>8</sup> The method of moments is the most straightforward, and is calculated as follows:

$$\text{sampling variance} = (\text{between-sample mean square} - \text{within-sample mean square})/n.$$

The corrected sampling mean square is the between-sample mean square, which estimates random variance due to both sampling and measurement, less the within-sample mean square, which is an accurate estimate of the measurement variance alone. The Klotz-Milton-Zacks estimator is more sophisticated and accurate for representing the mean squared terms. The estimator is calculated as follows:

$$\text{sampling variance} = \frac{1}{n} \left[ \frac{SS(A)}{h+1} - \frac{SS(E)}{h(n-1)} \right]$$

where  $SS(A)$  is the between-sample sum of squares and  $SS(E)$  is the within-sample sum of squares. The only difference between the Klotz-Milton-Zacks estimator and the method of moments is the degrees of freedom used to calculate the mean square terms.<sup>8</sup>

The corrected estimate of sampling variance is tested for significance using the  $F$  test along with the original within-sample mean square and the same critical value of  $F$ , as described above. If the corrected between-sample mean square is not significantly different from the within-sample mean square, then all variance in the sample set is due to random sampling and measurement variance. If the corrected between-sample mean square is significantly different from the within-sample mean square, then there is another source of variance in the samples.<sup>7</sup>

One-way ANOVA calculations with random-effect factor corrections are useful for drawing conclusions about the variability of GSR deposition around a gunshot wound. For an element to be useful for determining the presence of GSR, it must be reproducibly detected using ICP-MS (low measurement variance) and somewhat evenly

distributed around the entrance wound so that sampling the wound at any location will yield positive results (low sampling variance). Low levels of measurement and sampling variances demonstrate the element's utility for differentiating wounds shot with two different bullet types.

#### *2.4.2 Principal Components Analysis*

Principal components analysis (PCA) is a multivariate statistical procedure for reducing the amount of data in a dataset when there are correlations present within the data. A data matrix is created containing a list of all of the samples in the dataset and the amounts of all of the variables present in each sample. A covariance matrix is then calculated, which examines how the different variables relate to one another. For example, the covariance matrix will determine if two different variables always increase and decrease together in the same samples, meaning that they may be correlated. From the covariance values, linear combinations of variables that fluctuate similarly are calculated. These linear combinations are called eigenvectors, and are the principal components (PCs) of the analysis. Each eigenvector has an associated eigenvalue, which describes the amount of information contained in the eigenvector. Therefore, the higher the eigenvalue, the more valuable the eigenvector (PC) is for describing the overall variance in the dataset. The same number of PCs are calculated as the original number of variables in the dataset. Each PC is calculated to be orthogonal to the preceding PC and describes the next greatest amount of variance in the dataset. Principal component 1 is calculated to correlate the highest sources of variation in the dataset, PC2 is orthogonal to PC1 and correlates the next highest sources of variation, and so on. The result of PCA is

that the largest and most informative sources of variance in the dataset can now be examined using a smaller number of variables (i.e. two or three PCs), instead of all of the original data variables. This also allows simple visualization of data trends as two PCs, such as PC1 and PC2, may be plotted as the x- and y-axes of a single graph, called a scores plot, which illustrates most of the variance in the samples projected into two dimensions. Samples with similar chemical composition will cluster together and away from chemically dissimilar samples on the scores plot, allowing conclusions to be drawn about how samples relate to one another. A corresponding plot called a loadings plot displays the variables that are responsible for the variance described by each PC. Variables that fluctuate similarly in the same samples will be positioned in the same area of the loadings plot, allowing visualization of variable correlations. Again, PC1 is the x-axis and PC2 is the y-axis so that the position of a variable on the loadings plot corresponds to sample positioning on the scores plot.<sup>7</sup>

The following example illustrates the PCA procedures with respect to GSR element concentrations in tissue samples. The dataset would be composed of the abundances of several elements (variables) in numerous tissue samples of different types, such as unshot or shot with jacketed or non-jacketed ammunition (samples). Analyzing for trends in the abundances of elements in the different sample types individually can become tedious and time consuming. However, if correlations are present between element abundances and sample types, a new set of variables, the PCs, may be calculated. For example, if lead and antimony concentrations are always higher in tissue samples shot with non-jacketed ammunition compared to jacketed ammunition, and copper is always more concentrated in jacketed wound samples, a single PC is calculated to

represent this correlated variation. Linear combinations of elements that vary similarly in the covariance matrix are calculated as PCs that describe the correlations. The PCs with the largest eigenvalues describe the largest sources of variance in the different tissue samples. Then PC1 and PC2, the two eigenvectors that describe the greatest sources of variance, are plotted as scores and loadings plots [Figure 3.2]. Tissue samples with similar chemical composition will group together in one area of the scores plot and away from other tissue sample groupings. The elements combined into PC1 and PC2 that describe the highest sources of variance in the dataset are plotted in the loadings plot. Elements that vary in similar ways will be grouped together in the loadings plot. The element positions in the loadings plot correspond to sample positions in the scores plot. For example, if lead and antimony are positioned negatively on PC1 in the loadings plot, then samples shot with non-jacketed ammunition that have high levels of both of those elements will be positioned negatively on PC1 in the scores plot. Likewise, samples shot with jacketed bullets that have relatively low levels of lead and antimony and high levels of copper will be positioned away from the samples shot with non-jacketed ammunition and positively on PC1. The loadings plot shows the position of copper as positive on PC1, indicating that levels of copper vary inversely to levels of lead and antimony in this dataset.<sup>7</sup>

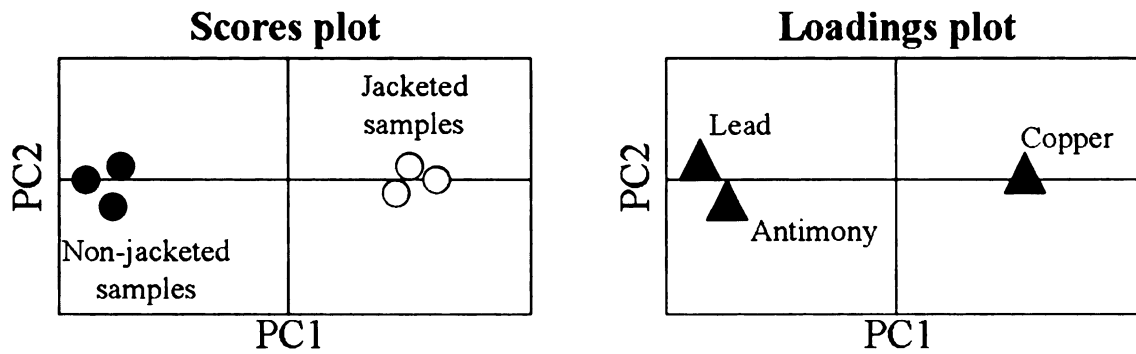


Figure 2.2 – Example results of PCA visualized as scores and loadings plots.

Principal components analysis reveals complex correlations between variables and samples that may not be discovered with univariate statistical methods. These correlations will be valuable for drawing conclusions about which elements are most useful for differentiating shot and unshot tissue as well as tissue samples shot with different ammunition types.



## **2.5 References**

1. Geneser F. Textbook of histology. Copenhagen: Munksgaard, 1986.
2. Kiernan JA. Histological & histochemical methods: theory and practice. 2<sup>nd</sup> ed. New York: Pergamon Press, 1990.
3. Masayoshi H, Yasuo S, Makie K, Hiroyoshi O. Mechanism of hematoxylin and eosin stains. *Journal of Analytical Bio-Science* 2003;26:377-83.
4. Lamble KJ, Hill SJ. Microwave digestion procedures for environmental matrices. *Analyst* 1998;123:103R-33R.
5. Skoog DA, Holler FJ, Nieman TA. Principles of instrumental analysis. 5<sup>th</sup> ed. Toronto: Thomson Learning, 1998.
6. deHoffmann E, Stroobant V. Mass spectrometry: principles and applications. 3<sup>rd</sup> ed. West Sussex: John Wiley & Sons, 2007.
7. Miller JN, Miller JC. Statistics and chemometrics for analytical chemistry. 5<sup>th</sup> ed. Harlow: Pearson Education Limited, 2005.
8. Miller, RG. Beyond ANOVA, basics of applied statistics. New York: John Wiley & Sons, 1986.

## **CHAPTER 3: MATERIALS AND METHODS**

### **3.1 Experimental Design and Sample Collection**

#### *3.1.1 Fresh Tissue Studies*

Two studies were conducted using fresh tissue samples. The first study was used to identify elements that were potentially useful in differentiating the two bullet types, as well as to assess variation in GSR composition within a wound. The second study was used to quantify the elements of interest to determine statistical differences in element concentrations between the two bullet types.

For the fresh tissue studies, two euthanized pigs (approximately 150 lbs each) were obtained from the Michigan State University (MSU) Swine Research Facility in June 2009. All pigs used in this research were treated in accordance with the MSU Institutional Animal Care and Use Committee (IACUC) guidelines. A certified firearms instructor from the MSU Campus Police shot both pigs seven times using a Smith & Wesson<sup>®</sup> .357 Magnum revolver. One pig was shot using 158 grain copper jacketed hollow point ammunition with a jacketed bullet base (Remington Arms Co. Inc., Lonoke, AR, Lot # B 17 HAS 502). The second pig was shot using 158 grain non-jacketed lead ammunition (Remington Arms Co. Inc., Lot # G 21 YB 6102). All shots were fired at a muzzle-to-target distance of 5 cm and the wounds were spaced approximately 10 cm apart to prevent cross contamination between wounds. The gun barrel and chamber were also cleaned between the different ammunition types. Immediately after all shots were fired, the wounds were collected by excising the tissue and underlying fat in an approximately 4 cm radius around each wound. Samples were also removed from these

wounds for histology analysis. The tissue samples were wrapped loosely in waxed paper, sealed in plastic bags, and stored at -80 °C until analysis.

In July 2009, one euthanized pig (approximately 100 lbs) was obtained from the MSU Swine Facility to serve as a control. Four samples of unwounded skin and underlying fat (approximately 20 cm x 20 cm each) were removed, packaged, and stored until analysis as described above.

For the first fresh tissue study, two shot tissue samples (one for each bullet type) and one control sample were used. Three tissue sections were removed from each gunshot wound and one section was removed from the control tissue sample. The tissue sections were microwave-digested and analyzed by ICP-MS, following procedures described below. For the second fresh tissue study, 10 shot tissue samples (five from each bullet type) and one control sample were used. One tissue section was taken from each sample, microwave-digested, and analyzed by ICP-MS, quantifying the elements of interest.

### *3.1.2 Sampling Study*

In June 2009, one euthanized pig (approximately 200 lbs) was obtained from the MSU Swine Research Facility. The pig was shot five times with the same firearm and non-jacketed ammunition used in the fresh tissue studies described above. All shots were fired at a muzzle-to-target distance of 5 cm and were spaced approximately 20 cm apart to prevent cross contamination between wounds. The gun barrel was cleaned after every shot to make GSR deposition as reproducible as possible. Immediately after all shots were fired, the wounds were collected by excising the tissue and underlying fat in an

approximately 8 cm radius around each wound. The wounds were packaged and stored until analysis as described above.

One wound was sampled for the study by excising tissue sections in four directions extending out from the entrance wound: 12 o'clock (12:00), 3 o'clock (3:00), 6 o'clock (6:00), and 9 o'clock (9:00) [Figure 3.1]. The tissue was sampled directly adjacent to the wound (0 cm) and every 2 cm out to the wound edge in each direction. The 19 tissue sections (five in each direction except 3:00, where the wound edge was at 6 cm) as well as three control tissue samples from the same control pig used in the fresh tissue studies were then microwave digested and analyzed by ICP-MS to quantify the elements of interest at each location around the wound.

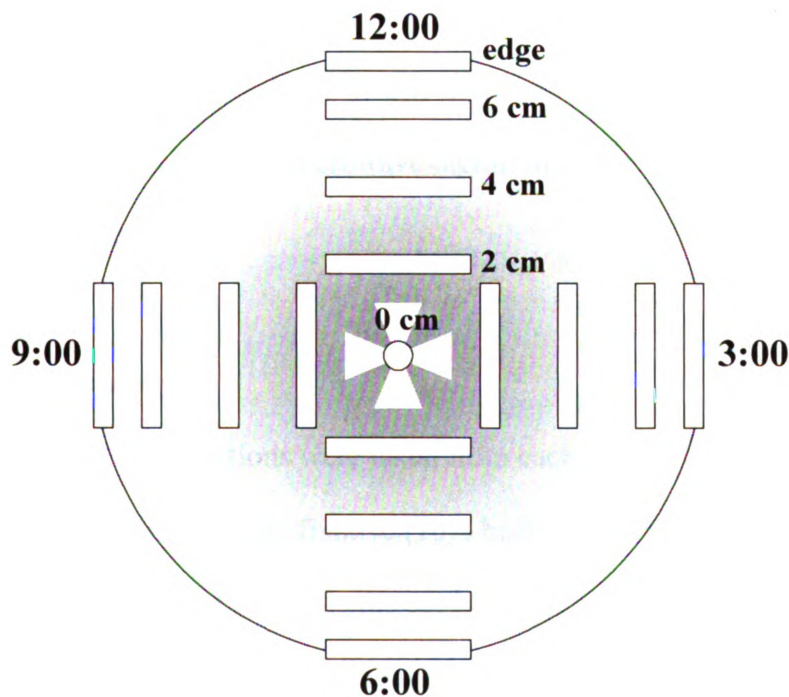


Figure 3.1 – Diagram of wound where tissue samples were excised for analysis.

### *3.1.3 Decomposition Study*

In October 2009, three euthanized pigs (approximately 150 lbs each) were obtained from the MSU Swine Research Facility. Control samples of tissue were removed from each pig before wounding. Two pigs were shot 12 times each with the same gun and ammunition as the fresh tissue studies. As before, one pig was shot with the jacketed ammunition and the second pig was shot with the non-jacketed ammunition. The gun barrel was cleaned after each shot, and the chamber was cleaned before reloading. All three pigs were then transported to a research field, where the unshot pig was stabbed 12 times to create open wounds to attract insect activity similar to the shot pigs. The pigs were placed inside separate wire cages to protect them from predators while still allowing exposure to the environment. The wounds and histology samples were collected over a period of 49 days, following procedures for excision, packaging, and storage described above. One tissue section was removed from each tissue sample (shot and control) for microwave digestion and ICP-MS analysis to quantify the elements of interest.

### **3.2 Histology**

Tissue sections were taken from each wound in the area of highest soot density and placed in formalin fixative (10% buffered for the fresh tissue wounds, Fisher Diagnostics Co. LLC, Kalamazoo, MI; 37% formaldehyde solution for the decomposed tissue wounds, Columbus Chemical Industries, Inc., Columbus, WI). The tissue sections were processed for hematoxylin and eosin (H & E) staining by the Hurley Medical Center Pathology laboratory according to the established and standard staining procedures of

that lab. Stained tissue sections were evaluated using a light microscope (Nikon Eclipse 50i equipped with a 2x-60x lens, Nikon Inc., Melville, NY).

### **3.3 Microwave Digestion of Porcine Tissue**

Tissue samples were removed from the -80 °C freezer and allowed to thaw prior to sample preparation. Skin directly adjacent to the wounds was removed from the underlying fat using a disposable scalpel. Between 0.35 and 0.5 g of each tissue sample were placed into acid and peroxide washed quartz vessels (Milestone, Inc., Shelton, CT). A 1 mL aliquot of hydrogen peroxide ( $\text{H}_2\text{O}_2$ , 30%, Columbus Chemical Industries, Inc.) and 2 mL Optima grade nitric acid ( $\text{HNO}_3$ , 69%, Fisher Scientific, Pittsburgh, PA) were added to each vessel. The quartz vessels were then capped and placed into larger Teflon<sup>TM</sup> vessels (Milestone, Inc.) that contained 10 mL Milli-Q water (Milli-Q Academic, Millipore, Billerica, MA) and 2 mL 30%  $\text{H}_2\text{O}_2$ . The Teflon<sup>TM</sup> vessels were then securely closed and placed into a Milestone Ethos EX microwave digester (Milestone, Inc.). Samples were digested using the following microwave temperature program: 15 minute temperature ramp from room temperature up to 210 °C, followed by a 10 minute hold at 210 °C. The microwave wattage was set at 1000 W to provide enough power to heat all vessels. Nine tissue samples and one procedural blank (prepared in the same way but without tissue present) were analyzed per microwave digestion run. The temperature probe was placed inside the procedural blank vessel, and the microwave system automatically adjusted the applied wattage to obtain and maintain the desired

temperature. The quartz vessels were cleaned after each tissue digestion by running procedural blanks and rinsing with distilled water before reuse.

After digestion, the tissue digests were allowed to cool to room temperature and diluted to 2% HNO<sub>3</sub> by adding 0.5 mL of the digest solutions to 11.168 mL Milli-Q water in 15 mL polypropylene conical tubes (Corning, Inc., Corning, NY). The dilution was necessary to prevent degradation of the polypropylene tubes and decrease the acid concentration for ICP-MS analysis. The remaining concentrated digest solutions were transferred to separate 15 mL polypropylene conical tubes for storage as well. Both the concentrated and diluted digest solutions were stored at 4 °C until ICP-MS analysis.

### **3.4 ICP-MS Analysis of Fresh Tissue Samples**

The seven tissue samples from the first fresh tissue study (three samples from one wound from each bullet type and one control sample) were analyzed using full mass scan mode to identify all elements present at significant levels. Prior to analysis, the diluted tissue digest solutions and procedural blanks were further diluted 1:10 (v/v) with 2% HNO<sub>3</sub> and spiked with 20 µg/L In and 20 µg/L Bi (SPEX CertiPrep, Inc., Metuchen, NJ) as internal standards. The solutions were analyzed by ICP-MS using a Micromass Platform quadrupole ICP-MS (now Thermo Fisher Scientific, Inc., Waltham, MA.) The instrument was equipped with a CETAC ASX-500 autosampler (CETAC Technologies, Omaha, NE), and a Dynolite<sup>TM</sup> detector with a -15 kV conversion dynode and electron multiplier. Instrument operating parameters are given in Table 3.1. The instrument was operated in full mass scan mode using MassLynx software (version 3.4, Waters Corp.,



Milford, MA). Digest samples and procedural blanks were analyzed in triplicate in random order. After sample injection, the injector was rinsed for 90 seconds with 2% HNO<sub>3</sub> to prevent sample carryover.

Table 3.1 – ICP-MS parameters for full mass scan and selected ion monitoring (SIM) analyses.

<b>ICP-MS Operating Parameters</b>	
RF power (W)	1350
Argon flow rates (L/min)	
Outer	13
Intermediate	0.8-0.95
Nebulizer	0.67-0.7
Sampling cone	Ni with Cu core, 1.14 mm diameter orifice
Cone Voltage (V)	100-125
Skimmer cone	Ni, 0.89 mm diameter orifice
MS resolution	Unit mass
Hexapole gas flow rates (mL/min)	
Helium	4-5
Hydrogen	2
Hex Bias (V)	-1.0-1.0
<b>Data Collection Parameters</b>	
Mode	Full Mass Scan or Selected Ion Monitoring (peak jumping)
Sample scan time (s)	75
Dwell time (s)	0.2 (SIM mode only)
Interchannel delay time (s)	0.020 (SIM mode only)
<b>Autosampler Parameters</b>	
Sample read delay (s)	105
Rinse time (s)	90

Instrument responses for elements below atomic mass 155 were normalized to <sup>115</sup>In, and elements with atomic weights above 155 were normalized to <sup>209</sup>Bi. Dilution

factors were taken into account and concentrations of all elements were expressed as  $\mu\text{g}$  element/ g tissue for comparison.

### **3.5 Statistical Treatment of Fresh Tissue Data**

All statistical analyses were performed using Microsoft Excel 2003 (Microsoft<sup>®</sup> Corp., Redmond, WA). The average elemental concentration ( $\mu\text{g/g}$  tissue) was calculated for each bullet type (three samples analyzed in triplicate from each wound, giving  $n = 9$ ), the control sample (triplicate analyses,  $n = 3$ ), and the procedural blank sample (triplicate analyses,  $n = 3$ ). The limit of detection (LOD), defined as three times the standard deviation of the procedural blank concentration, was calculated for each element, as well as the ratio of the average procedural blank concentration to the lowest concentration in a shot tissue sample from either bullet type. The relative standard deviation (RSD) was calculated for each element in each bullet type, and the Grubbs' test for statistical outliers was performed on all elements that had RSDs higher than 15%.<sup>1</sup> For all elements, any data points determined to be outliers at the 95% confidence level were removed. Elements with an RSD greater than 15% in both bullet types after removing statistical outliers were eliminated from the suite of potentially useful elements.

Analysis of variance (ANOVA) at the 90% confidence level ( $p \leq 0.1$ ) was used to assess significant differences in element concentrations between-wounds and within-wounds, using triplicate analyses of three tissue samples from each bullet type. The null hypotheses were that there was no difference in the elemental concentrations of replicates from the same sample and that there was no difference in the elemental concentrations of samples taken from the same wound. The alternate hypotheses were that the elemental

concentrations of replicates and between samples taken from the same wound were not equal. Random effect corrections were applied to between-sample variances to correct for the random nature of sampling the tissue for analysis, when appropriate.<sup>2</sup>

Student's *t*-tests were also performed to compare the average concentration of each element between the two bullet types. The calculated *t*-statistic for each element was compared with statistical tables of critical *t*-values at the 95% and 99% confidence limits (two-tail) to assess statistical differences in element concentrations.

### **3.6 ICP-MS Quantitation of Fresh and Decomposed Tissue Samples**

The 11 tissue samples from the second fresh tissue study (one sample from five wounds for each bullet type and one control), tissue samples from the decomposition study ( $n = 38$ ), and all tissue samples from the sampling study ( $n = 22$ ) were analyzed using selected ion monitoring (SIM) mode for the selected elements of interest to increase sensitivity. The instrument tune conditions were optimized daily using a 10 µg/L solution of Be, Co, In, Ce, Bi, and U (SPEX CertiPrep, Inc.) prepared in a 2% HNO<sub>3</sub> solution. Ten multi-element external calibration standards containing the elements of interest were prepared from stock standard solutions of each element (1000 mg/L each; P, K, Fe, Cu, Sb, Ba, and Pb from SPEX CertiPrep, Inc.; Mg and Zn from Thermo Fisher Scientific, Inc.) The stock solutions were diluted with 2% HNO<sub>3</sub> to concentrations ranging from 0.1-500 µg/L, with all elements having equal concentrations in each standard solution. Each standard solution was spiked with 20 µg/L In and 20 µg/L Bi as

internal standards prior to ICP-MS analysis. Calibration standards were analyzed in order from low to high concentration to minimize carry-over effects.

Standard Reference Material 1643e (SRM, National Institute of Standards and Technology, Gaithersburg, MD) was analyzed to assess instrument accuracy during sample analyses as the standard contained known concentrations of all elements of interest. The SRM was diluted 1:10 (v/v) with 2% HNO<sub>3</sub> and spiked with 20 µg/L In and 20 µg/L Bi internal standards prior to ICP-MS analysis.

Due to the large range in concentrations for the different elements in shot tissue samples, it was necessary to prepare the tissue digest samples at two different dilution levels. After microwave digestion, the digest solutions (fresh tissue, decomposed tissue, control tissue, and procedural blank) were diluted to 2% HNO<sub>3</sub> as described previously. One sample set was not further diluted (hereafter referred to as ‘undiluted’) prior to being spiked with 20 µg/L In and 20 µg/L Bi as internal standards. A second sample set was prepared by further diluting the digests 1:100 (v/v) with 2% HNO<sub>3</sub> (hereafter referred to as ‘diluted’). The diluted digests were then spiked with 20 µg/L In and 20 µg/L Bi as internal standards.

The undiluted and the diluted digests were analyzed by ICP-MS using the same instrument system described previously with additional parameters for SIM mode analysis, as detailed in Table 3.1. Sets of calibration standards were analyzed at the beginning of an analysis and after approximately every 30 samples to account for instrument drift. Samples were analyzed in the following order for all studies: calibration standard set, SRM, diluted digests and procedural blanks randomized, SRM, calibration

standard set, SRM, undiluted digests and procedural blanks randomized, SRM, calibration standard set. After each sample injection, the injector was rinsed for 90 seconds with 2% HNO<sub>3</sub>, and two additional 2% HNO<sub>3</sub> rinses were performed between each set of samples.

The resulting instrument responses were quantitated using MassLynx software. Instrument responses for <sup>24</sup>Mg, <sup>31</sup>P, <sup>39</sup>K, <sup>56</sup>Fe, <sup>63</sup>Cu, and <sup>64</sup>Zn were normalized to <sup>115</sup>In, and <sup>121</sup>Sb, <sup>138</sup>Ba, and <sup>208</sup>Pb were normalized to <sup>209</sup>Bi. Element concentrations in the tissue samples were determined from the average of the linear calibration curves run immediately before and after the digest sample set to be quantified. Element concentrations in each tissue digest were corrected for dilution factors and normalized to the original tissue mass to yield final element concentrations that were expressed as µg element/ g tissue.

### **3.7 Principal Components Analysis of Decomposition Study Data**

Principal components analysis (PCA) was performed using SIMCA-P software (version 11.5, Umetrics Inc., San Jose, CA). The data matrix included the concentrations (µg element/g tissue) of the five elements of interest (<sup>56</sup>Fe, <sup>63</sup>Cu, <sup>121</sup>Sb, <sup>138</sup>Ba, and <sup>208</sup>Pb) in each sample in the decomposition study (procedural blanks, control stab wounds, wounds shot with jacketed ammunition, and wounds shot with non-jacketed ammunition) determined using ICP-MS quantitation. Only samples collected on days 0, 5, 14, 24, 34, and 44 were included as the element concentrations did not vary greatly throughout decomposition. The element concentrations were mean-centered and

univariate scaled prior to PCA, which are common data pretreatment procedures. Mean-centering shifted the concentrations of the elements so that the means were centered at the origin, which makes results interpretation more straightforward. The element concentrations were univariate scaled so that the elements present in large abundance would not dominate the analysis and undervalue the low abundance elements in terms of their ability to differentiate between the tissue samples as well.

Principal components analysis was performed to examine the systematic variation of element concentrations in the decomposition study samples and to visualize the differentiation of samples shot with different bullet types. Principal component 1 (PC1) was plotted versus PC2 as these components described the elements that varied the most among the different tissue sample types. The corresponding loadings plot of PC1 versus PC2 was examined to determine which elements varied between the different sample types and were responsible for associating and discriminating sample groupings in the scores plot.

### **3.8 References**

1. Miller JN, Miller JC. Statistics and chemometrics for analytical chemistry. 5<sup>th</sup> ed. Harlow: Pearson Education Limited, 2005.
2. Miller, RG. Beyond ANOVA, basics of applied statistics. New York: John Wiley & Sons, 1986.

## **CHAPTER 4: RESULTS AND DISCUSSION**

### **4.1 Introduction**

The differentiation of two bullet types based on gunshot residue (GSR) was first investigated using fresh porcine tissue. One pig was shot with jacketed ammunition and two pigs were shot with non-jacketed ammunition. The wounds were collected, microwave digested, and analyzed using inductively coupled plasma mass spectrometry (ICP-MS) to determine elemental content. Elements in addition to those already considered characteristic of GSR (antimony (Sb), barium (Ba), and lead (Pb)), were identified in order to increase confidence in gunshot wound determination. The ability of ICP-MS to differentiate the two bullet types using their element profiles was also investigated. A sampling study was used to investigate the spatial pattern of GSR deposition around a fresh non-jacketed bullet wound. Finally, to make the results more applicable in a forensic setting, the effects of moderate decomposition on the ability to detect GSR and differentiate bullet types were also assessed.

### **4.2 Fresh Tissue Sample Observations and Histology Results**

Dense soot deposition was visible in the wound tract and around the immediate perimeter of wounds made by both the jacketed and non-jacketed bullets [Figure 4.1]. Wound edges were darkened, exhibiting typical characteristics of a close-range gunshot wound. No stippling was observed because the pigs were euthanized prior to being shot. Microscopic examination of the wounds revealed soot staining in the epidermis. Histology results after hematoxylin and eosin (H & E) staining showed the expected thermal artifact associated with gunshot wounds (i.e. homogenization of the epidermis



with streaming nuclei) in both bullet types, as well as dark granules of burned gunpowder and refractive particles of unburned gunpowder [Figure 4.1]. There were slight differences in soot deposition patterns and histology results between the two ammunition types due to different types and amounts of gunpowder, but this was not a feature of the study.

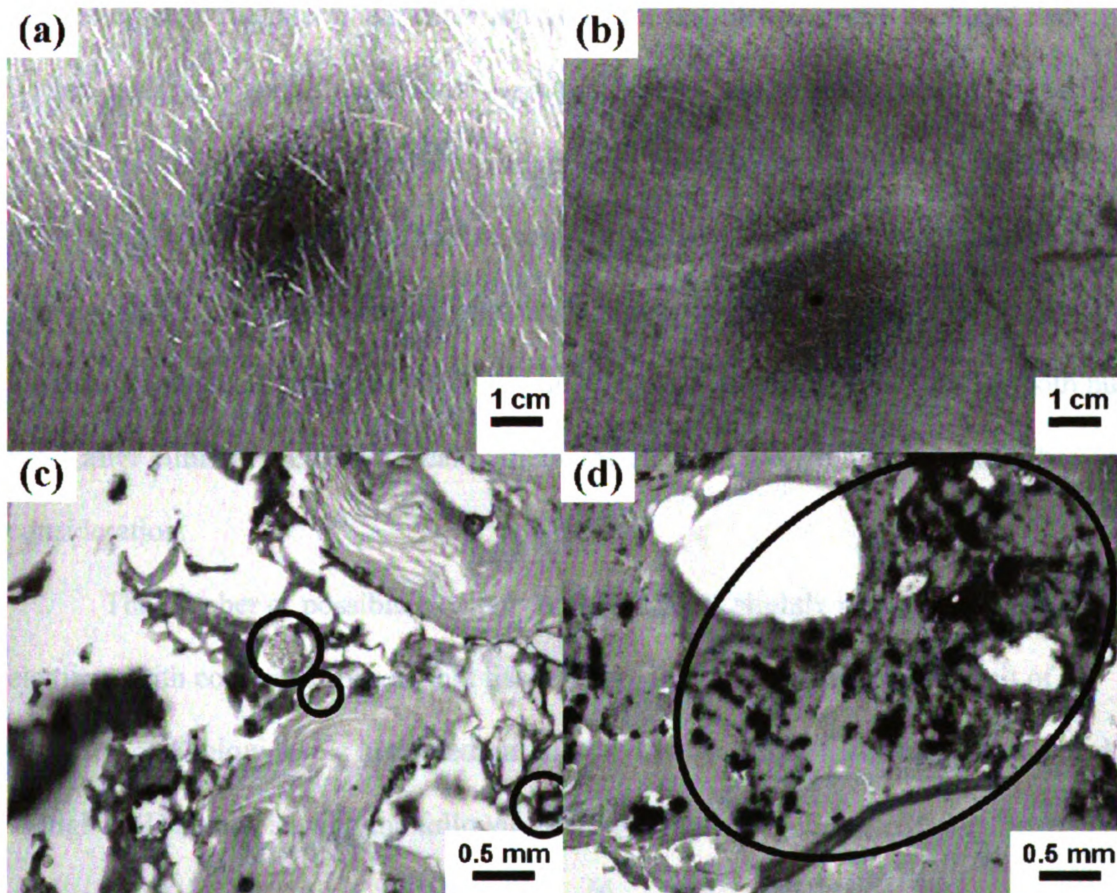


Figure 4.1 - Gunshot wounds in fresh porcine tissue from (a) jacketed bullets and (b) non-jacketed bullets, along with corresponding micrographs of H & E stained histology results (c and d, respectively). Refractive particles of unburned gunpowder are circled in the jacketed bullet wound histology slide (c), and dark granules of burned gunpowder are circled on the non-jacketed bullet wound histology slide (d).

### 4.3 Selection of Elements to Discriminate Bullet Types

The full mass scan ICP-MS analyses detected many potentially useful elements in the fresh tissue digest samples. Element concentrations from ICP-MS analyses were analyzed using a series of statistical procedures to select those elements most useful for differentiating shot from unshot tissue as well as differentiating the two bullet types. First, elements with average concentrations in tissue samples shot with both bullet types that were below the instrument detection limits for that element were excluded from further analyses. Next, if the ratio of the average procedural blank concentration to the lowest concentration in a shot tissue sample from either bullet type was greater than 30%, the element was excluded from further consideration since more than one third of the element signal was due to sample preparation and/or instrument contamination. Finally, if the relative standard deviation (RSD) for an element was greater than 15% for both bullet types after elimination of statistical outliers, the element was excluded from further consideration.

The number of possible elements of interest was slightly reduced by excluding elements with concentrations in shot tissue samples below the instrument limit of detection and below levels in procedural blanks. Many elements were also excluded due to high RSD levels, leaving the following elements as potentially useful for discrimination:  $^{24}\text{Mg}$ ,  $^{31}\text{P}$ ,  $^{39}\text{K}$ ,  $^{56}\text{Fe}$ ,  $^{63}\text{Cu}$ ,  $^{66}\text{Zn}$ ,  $^{121}\text{Sb}$ ,  $^{138}\text{Ba}$ , and  $^{208}\text{Pb}$ . It should be noted that the RSDs for  $^{121}\text{Sb}$ ,  $^{138}\text{Ba}$ , and  $^{208}\text{Pb}$  were higher than 15% in both bullet types due to the high concentrations of these elements in the samples. However, the three elements were included in subsequent analyses since they are currently considered to be characteristic of GSR.

One-way analysis of variance (ANOVA) was applied to the three tissue samples analyzed in triplicate from each bullet type to identify those elements that showed significant differences within and between wounds at the 90% confidence level ( $p \leq 0.1$ ). At this  $p$ -value, the probability that the elemental concentrations were the same was 10% or less. The variation was not significant among replicates of the same sample, as expected due to the high precision of ICP-MS. In addition, and for both bullet types, there was no significant difference in concentrations for samples taken from the same wound for the following elements:  $^{24}\text{Mg}$ ,  $^{31}\text{P}$ ,  $^{39}\text{K}$ ,  $^{56}\text{Fe}$ ,  $^{63}\text{Cu}$ , and  $^{66}\text{Zn}$ . There was significant between-sample variance in element concentration for  $^{121}\text{Sb}$ ,  $^{138}\text{Ba}$ , and  $^{208}\text{Pb}$  in samples from jacketed bullet wounds, and in  $^{138}\text{Ba}$  and  $^{208}\text{Pb}$  for non-jacketed bullet wounds. However, this variation was due to high concentrations of those elements in the wound samples. In subsequent analyses, the digests were further diluted prior to quantitation.

Finally, to test whether the elements of interest could be used to differentiate the two bullet types, the Student's  $t$ -test was used to compare the mean element concentrations in each [Figure 4.2]. Elements with significant differences in concentration at the 95% confidence level and above were considered useful for differentiating the two bullet types. Concentrations of  $^{24}\text{Mg}$ ,  $^{31}\text{P}$ ,  $^{39}\text{K}$ ,  $^{63}\text{Cu}$ , and  $^{66}\text{Zn}$  were significantly higher in wounds shot with jacketed bullets (99% confidence level), the elements  $^{121}\text{Sb}$  and  $^{208}\text{Pb}$  were significantly more concentrated in wounds shot with non-jacketed bullets (99% confidence level), and  $^{56}\text{Fe}$  and  $^{138}\text{Ba}$  concentrations were not

significantly different between the two bullet types. All elements were also confirmed to be useful for differentiating shot from unshot tissue by comparison of the mean element concentrations in a similar manner.

Thus, the suite of elements considered potentially useful for differentiating shot from unshot tissue and differentiating the two bullet types consisted of  $^{24}\text{Mg}$ ,  $^{31}\text{P}$ ,  $^{39}\text{K}$ ,  $^{56}\text{Fe}$ ,  $^{63}\text{Cu}$ ,  $^{66}\text{Zn}$ ,  $^{121}\text{Sb}$ ,  $^{138}\text{Ba}$ , and  $^{208}\text{Pb}$ . These elements could originate from the ammunition primer, gunpowder, cartridge case, or the bullet itself, as well as from the gun barrel.<sup>1</sup> The three elements currently considered characteristic of GSR, Sb, Ba, and Pb, come from the primer, and Pb and Sb could also come from the bullet. Copper, zinc (Zn), and nickel (Ni) are known materials in bullet jackets and cartridge cases. However, since the sampling cone of the ICP-MS was composed of Ni, data for that element are not reliable in this study, and the element was not considered in analyses. The gun barrel used in these studies was made of stainless steel, which is mainly composed of Fe. Magnesium (Mg) and phosphorus (P) are likely oxidizers in the gunpowder, and potassium (K) may come from the synthesis of the gunpowder. Further analyses are required to determine the complete chemical composition of the ammunition as this was not the focus of the current study.

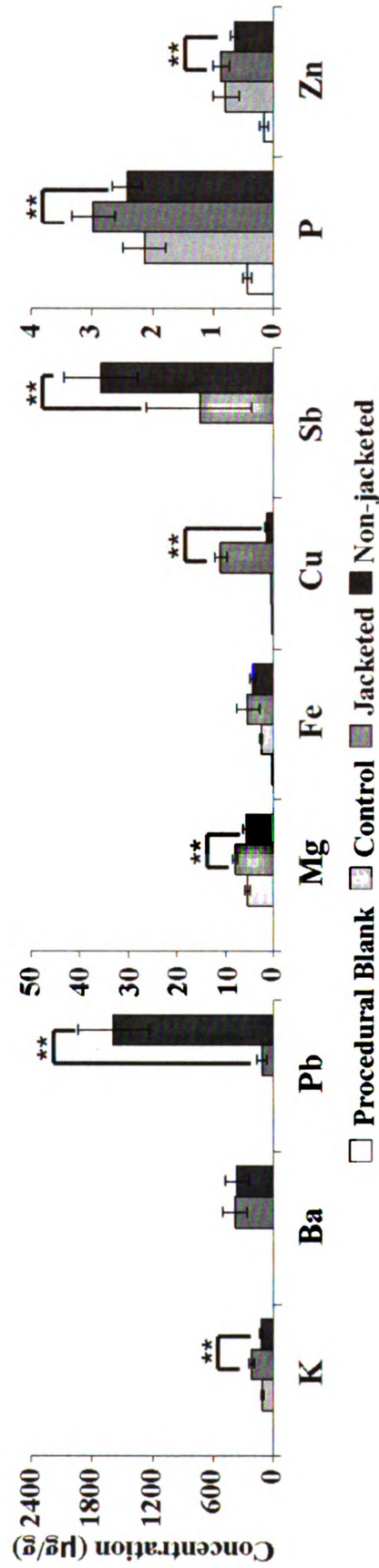


Figure 4.2 – Mean concentrations of elements of interest in the first fresh tissue study (procedural blank n = 3, control n = 3, jacketed n = 9, and non-jacketed n = 9). The error bars represent one standard deviation. Significant difference between element concentrations at 99% confidence level ( $p \leq 0.01$ ) are indicated by \*\*.

#### 4.4 Quantitation of Elements in Fresh Tissue Samples

At this stage, nine elements ( $^{24}\text{Mg}$ ,  $^{31}\text{P}$ ,  $^{39}\text{K}$ ,  $^{56}\text{Fe}$ ,  $^{63}\text{Cu}$ ,  $^{66}\text{Zn}$ ,  $^{121}\text{Sb}$ ,  $^{138}\text{Ba}$ , and  $^{208}\text{Pb}$ ) were identified as being potentially useful for differentiating shot from unshot tissue as well as differentiating bullet type. The levels of these elements in the fresh tissue samples (one control, five shot with jacketed bullets, and five shot with non-jacketed bullets) were then quantitated by ICP-MS. However, the elements  $^{24}\text{Mg}$ ,  $^{31}\text{P}$ , and  $^{39}\text{K}$  were subsequently eliminated from consideration due to nonlinear calibration curves as a result of high background levels in the instrument. Limits of quantitation for the remaining elements were determined as the concentration of the lowest linear point on the calibration curve or listed as less than the lowest standard concentration analyzed [Table 4.1]. Koons reported that concentrations of Sb, Ba, and Pb typically observed in GSR were 40-500 ng.<sup>2</sup> The limits of quantitation determined for this study are between one and three orders of magnitude lower than levels expected in GSR for those three elements, indicating that the instrument was capable of detecting elements present in GSR. The mean concentrations for all six elements of interest in the four standard reference material (SRM) samples were calculated and compared to the reported concentrations in the material [Table 4.1]. The percent error between the true and observed Zn concentrations was 25% and hence, Zn was excluded from further consideration. Errors for the remaining five elements (Fe, Cu, Sb, Ba, and Pb) were all less than 10%, indicating that the ICP-MS was accurately quantifying the elements and hence, one analysis of each digest sample was sufficient.



Table 4.1 – Limits of quantitation (LOQs) and SRM recovery results for elements of interest in the fresh tissue study.

Element	LOQ (µg/L)	SRM Average % Error
<sup>56</sup> Fe	5	7
<sup>63</sup> Cu	5	1
<sup>66</sup> Zn	10	25
<sup>121</sup> Sb	< 0.1	2
<sup>138</sup> Ba	0.5	6
<sup>208</sup> Pb	0.25	3

Both the undiluted and diluted tissue digest sample sets were analyzed. The elements <sup>56</sup>Fe and <sup>66</sup>Zn were quantified in the undiluted digests due to the low concentrations of these elements observed in the first fresh tissue study. The remaining four elements (<sup>63</sup>Cu, <sup>121</sup>Sb, <sup>138</sup>Ba, and <sup>206</sup>Pb) were one to three orders of magnitude more concentrated and were quantified using the diluted digests. This was necessary to avoid detector saturation and to ensure that the instrument responses were within the linear range of the calibration curve for those elements.

A comparison of mean elemental concentrations in all tissue samples analyzed for each bullet type, as well as procedural blank and control tissue samples, is shown in Figure 4.3. The mean element concentrations in tissue samples shot with either bullet type are considerably higher than the corresponding procedural blank and control tissue sample concentrations for all five elements of interest, indicating that all elements can be used to differentiate shot from unshot tissue. The Student's *t*-test was used to test for significant differences in the mean element concentrations between jacketed and non-

jacketed bullet wounds. There were significant differences between the two bullet types in the Sb and Pb concentrations at the 99% confidence level and in the Cu concentrations at the 95% confidence limit. Antimony and Pb were both more concentrated in tissue shot with non-jacketed bullets, with mean concentrations of 5444 and 147565  $\mu\text{g/g}$ , respectively, compared to 1732 and 6567  $\mu\text{g/g}$  in wounds shot with jacketed ammunition. Copper was more concentrated in tissue shot with jacketed ammunition, with a mean concentration of 2524  $\mu\text{g/g}$  compared to 123  $\mu\text{g/g}$  in wounds shot with non-jacketed bullets. These elements most likely originate from the bullets themselves, since the jacketed bullets have Cu jackets and the non-jacketed bullets are composed of Pb and possibly Sb. These three elements (Cu, Sb, and Pb) are therefore useful for differentiating the two bullet types in fresh gunshot wounds.



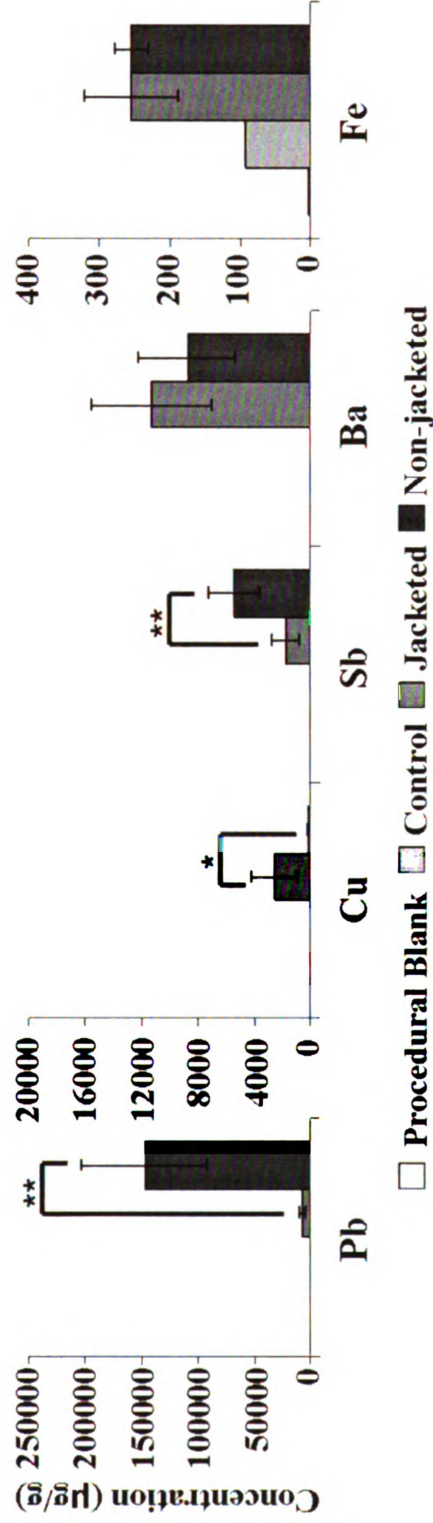


Figure 4.3 – Mean concentrations of elements of interest quantified in fresh tissue samples (procedural blank n = 6, control n = 1, jacketed n = 5, and non-jacketed n = 5). The error bars represent one standard deviation. Significant difference between element concentrations at 95% confidence level ( $p \leq 0.05$ ) are indicated by \* and significant difference between element concentrations at 99% confidence level ( $p \leq 0.01$ ) are indicated by \*\*.

Mean Fe and Ba concentrations were not significantly different between the two bullet types, possibly due to the fact that these elements originate from the interior of the gun barrel or the ammunition primers, which are more similar in elemental composition between the two ammunition types. Thus, all five elements of interest (Fe, Cu, Sb, Ba, and Pb) were successful in differentiating shot from unshot tissue, and three elements (Cu, Sb, and Pb) were capable of differentiating jacketed and non-jacketed bullet wounds in fresh tissue samples.

#### **4.5 Sampling Study Tissue Observations**

One fresh wound shot with non-jacketed ammunition was selected for the sampling study to investigate the distribution of GSR around the wound. The gunshot wound had similar characteristics to all other wounds shot with non-jacketed ammunition [Figure 4.8]. The gun was fired using a wire hanger as a support, which left the horizontal void in the GSR pattern that is apparent in Figure 4.8. There was a dense area of soot deposition around the entrance wound extending approximately 1 cm in all directions around the wound. A secondary ring of finer GSR deposition was also present, extending approximately 6 cm from the wound. This secondary ring of GSR, which was likely from the gap between the gun chamber and barrel, was visually heterogeneous, appearing more concentrated in the 6 o'clock (6:00) and 9 o'clock (9:00) positions compared to the 12 o'clock (12:00) and 3 o'clock (3:00) positions. There was also some blood staining on the tissue surface, which was most evident in the 9:00 direction. The edge of the wound was at slightly different distances from the center of the gunshot wound in each direction: 6.75 cm in the 12:00 direction, 6 cm in the 3:00 direction, 6.5 cm in the 6:00 direction,

and 7.5 cm in the 9:00 direction. The outermost edges of the wound did not appear to have any GSR present.

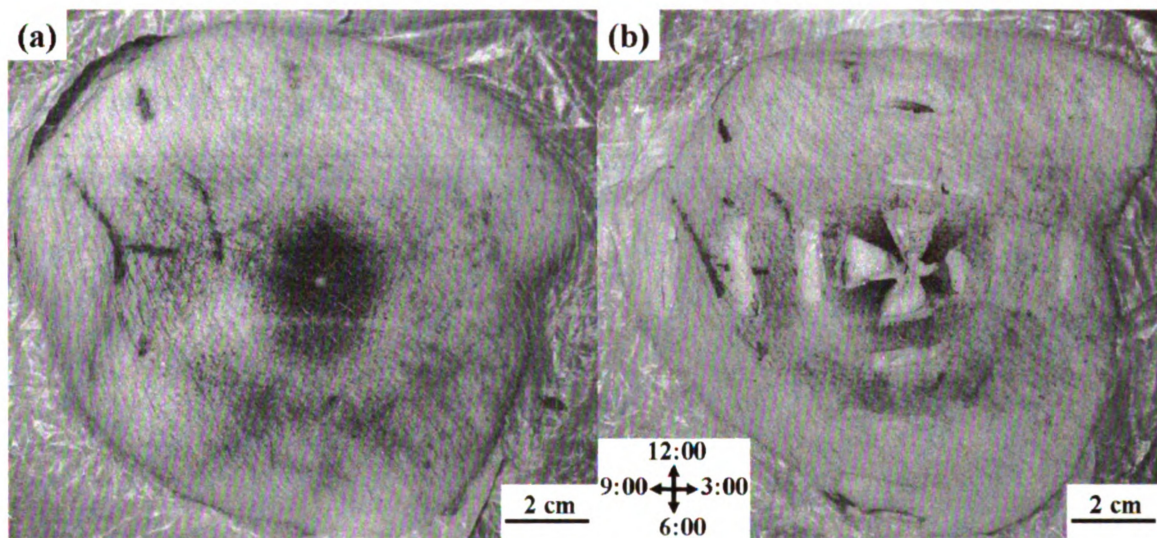


Figure 4.4 – Sampling study wound (a) before tissue sections were removed and (b) after tissue samples had been removed for analysis. The four directions that the tissue was sampled are indicated with arrows.

#### 4.6 Quantitation of Elements in Sampling Study Tissue Samples

The five elements of interest ( $^{56}\text{Fe}$ ,  $^{63}\text{Cu}$ ,  $^{121}\text{Sb}$ ,  $^{138}\text{Ba}$ , and  $^{208}\text{Pb}$ ) were quantitated using ICP-MS, and the limits of quantitation are listed in Table 4.2. The mean concentrations of the five elements in the four SRM samples were calculated and compared to the reported concentrations, as described previously [Table 4.2]. The percent error between the true and observed Cu concentrations was 20% and hence, Cu was excluded from consideration during this study. This was reasonable given that Cu levels were not expected to be useful for GSR determination around a non-jacketed bullet

wound. For all other elements, errors were less than 10%, indicating the instrument was accurately quantitating the elements in all samples.

Table 4.2 – Limits of quantitation (LOQs) and SRM recovery results for elements of interest in the sampling study.

Element	LOQ (µg/L)	SRM Average % Error
<sup>56</sup> Fe	5	3
<sup>63</sup> Cu	0.5	20
<sup>121</sup> Sb	0.5	1
<sup>138</sup> Ba	0.25	7
<sup>208</sup> Pb	0.25	2

Element concentrations were expected to decrease as the sampling distance from the entrance wound increased, so all element signals were monitored in both the undiluted and diluted tissue sample sets. Since <sup>56</sup>Fe was present in relatively low levels in the fresh tissue study, it was quantitated using the undiluted digest samples so that signals remained within the linear range of the calibration curve. The elements <sup>121</sup>Sb, <sup>138</sup>Ba, and <sup>208</sup>Pb were more concentrated and were quantitated in the diluted samples to ensure that sample signals were within the linear calibration curve range and did not saturate the detector.

The concentration of each element of interest in all shot tissue samples was compared to the concentration in the procedural blank and control tissue samples [Figure 4.5]. Since there was only one sample taken from each position around the wound, no



statistical measures of significant differences in concentrations could be made for the shot tissue samples.

Figure 4.5 – Concentrations of (a) Fe, (b) Sb, (c) Ba, and (d) Pb quantitated in the sampling study samples (procedural blank n = 3, control n = 3, and non-jacketed n = 1). Error bars are one standard deviation. In the 3:00 direction data, “6 cm/edge” indicates that the wound edge was at 6 cm.

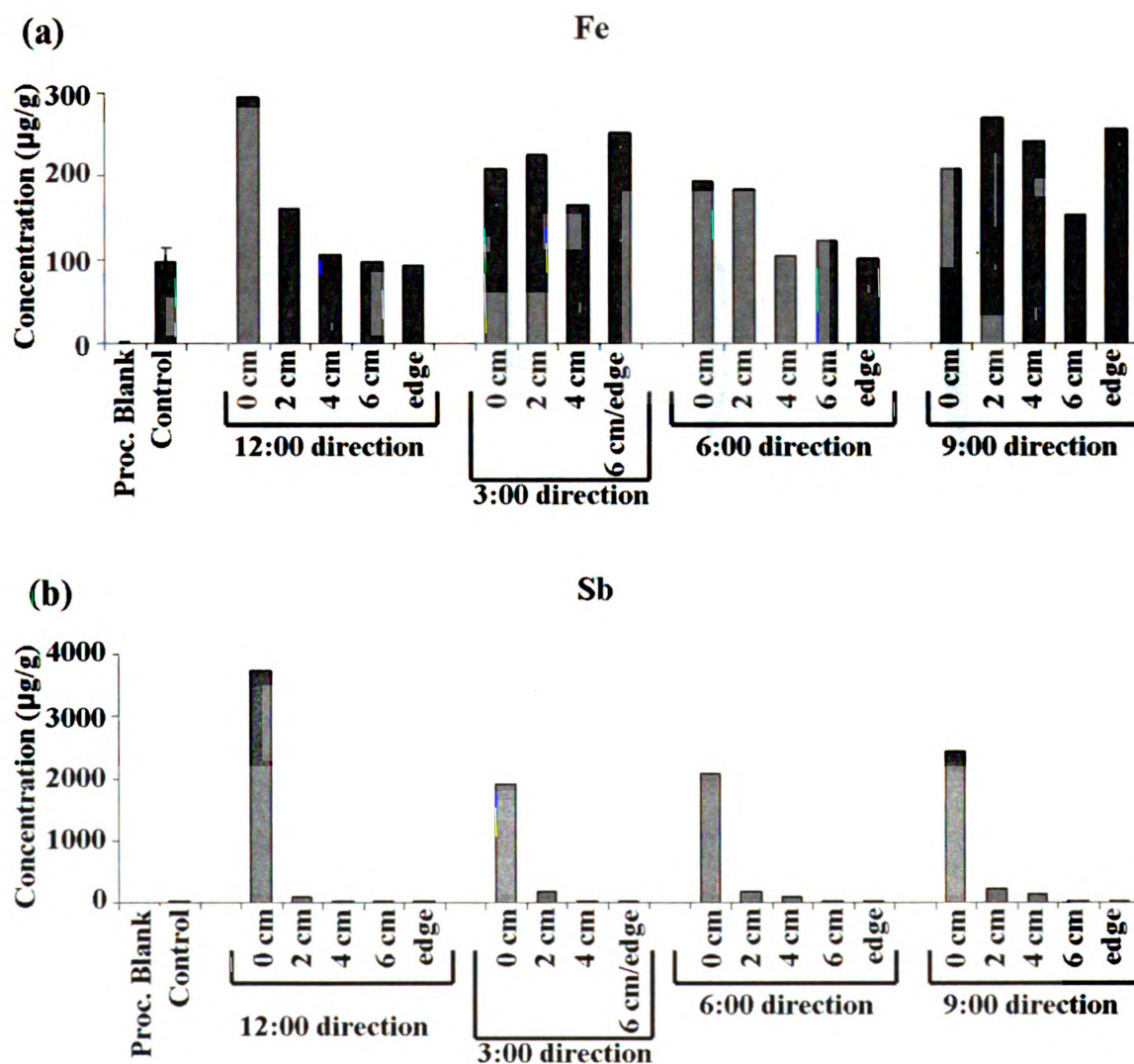
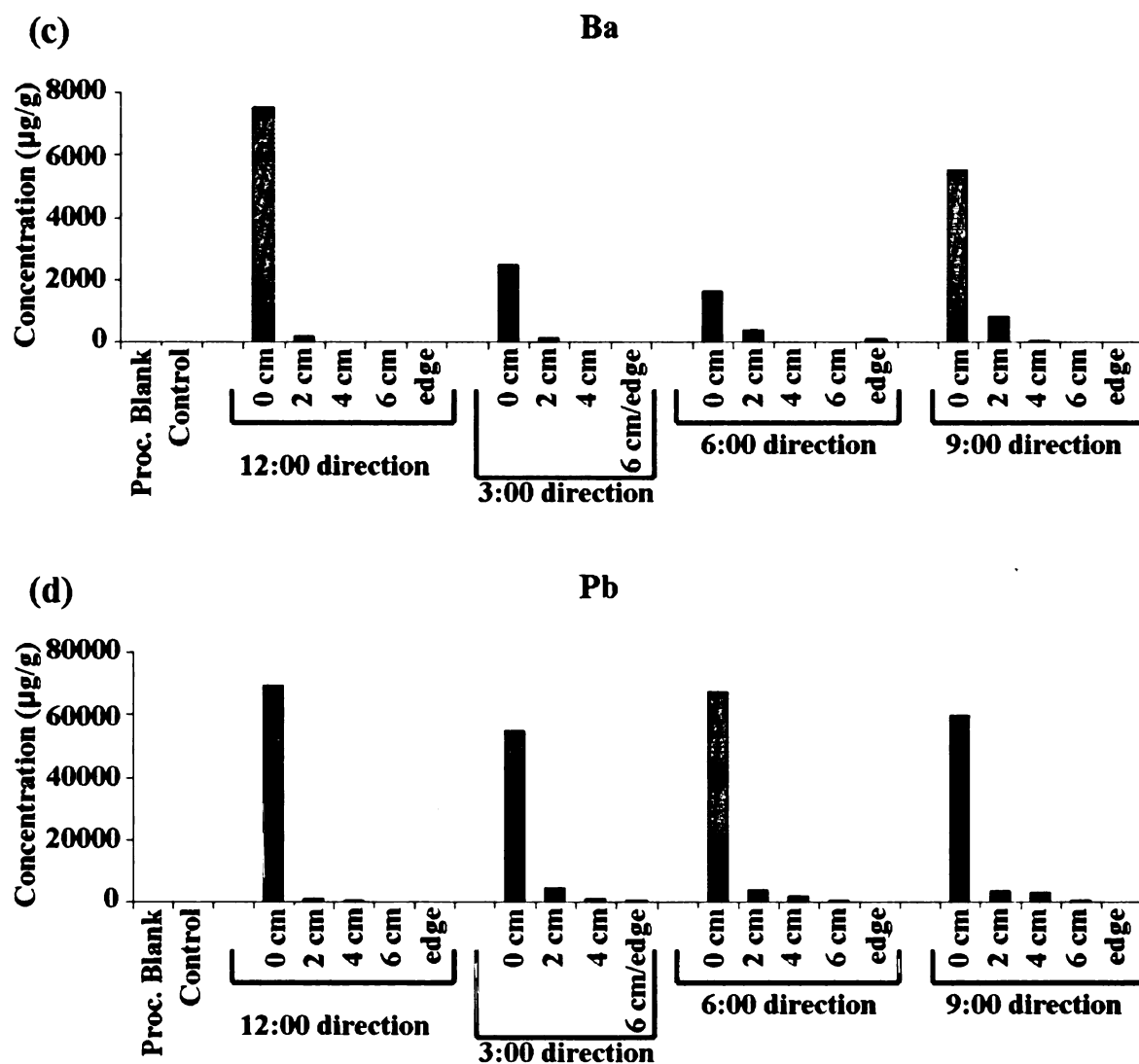


Figure 4.5 – Continued



A summary of the distances from the entrance wound that each element was detected above the concentration in the procedural blanks and control samples is shown in Table 4.3.

Table 4.3 – Summary of distances that elements of interest in shot tissue samples were detected at higher levels than procedural blank and control tissue samples.

<b>Element</b>	<b>Farthest Distance Element Detected</b>			
	<b>12:00</b>	<b>3:00</b>	<b>6:00</b>	<b>9:00</b>
Fe	2 cm	edge	2 cm	edge
Sb	2 cm	4 cm	edge	edge
Ba	edge	2 cm	2 cm	4 cm
Pb	edge	edge	edge	edge

The concentrations of Sb, Ba, and Pb were all highest directly adjacent to the wound, in the area of dense soot deposition, in all directions. The concentrations of these three elements then decreased in all four directions, with the distance that each element was last detected above concentrations in procedural blank and control samples varying for each element. Lead was present in shot tissue samples in concentrations at least one order of magnitude higher than the procedural blank and control samples all the way out to the wound edge in all four directions, indicating that Pb spread the farthest from the entrance wound, possibly because it was the most concentrated element in the GSR. Antimony was present out to the wound edge in the 6:00 and 9:00 directions, which were the same directions with the farthest spread of visual GSR, and only a few centimeters in the 12:00 and 3:00 directions. The Ba and Fe results were more difficult to interpret, as Ba was deposited farthest out in the 12:00 direction, and Fe was detected furthestmost in the 3:00 and 9:00 directions. The Fe results could be due to the presence of blood on the surface of the tissue, especially in the 9:00 direction, as blood contains Fe. These results indicate that the optimal sampling position to detect all elements characteristic of GSR by ICP-MS is directly adjacent to the wound and as far out as 2 cm from the entrance wound

in any direction. The high degree of GSR deposition variability from 2 cm outward could prevent detection of characteristic elements and not allow a wound to be definitively determined as a gunshot wound.

Overall, these fresh tissue studies allowed the expansion of the list of elements considered to be characteristic of GSR by adding Fe and Cu to Sb, Ba, and Pb, which are currently considered characteristic of GSR. The addition of these two elements increases confidence in GSR determination, as it is unlikely that these five elements would all be present on a surface due to other materials. Knowledge of the sample position most likely to produce conclusive results for the presence of GSR (adjacent to the entrance wound out to 2 cm) is also essential for coroners, medical examiners, and forensic pathologists. While these results were promising, the effect of decomposition on element concentrations was investigated to evaluate the practicality of this method for forensic applications.

#### **4.7 Decomposition Study Observations and Histology Results**

Gunshot wounds from both jacketed and non-jacketed bullets collected on day 0 of the decomposition study were visually very similar in appearance to those from the fresh tissue studies [Figures 4.6 and 4.7]. This observation was expected as wounds were inflicted using the same weapon and ammunition as in the previous studies. During the 49 day sample collection period, temperatures ranged from a high of 70 °F (day 37) to a low of 22 °F (day 41). Appreciable rainfall occurred on days 0, 4, 7, 19, 20, 21, 28, 47, and 48. Full details of the weather conditions are located in the Appendix.<sup>3</sup>



There was minimal insect activity during the first week of the study due to cool temperatures and rain. Bloating was evident and wounds were seeping on all pigs by day 19. By day 24, the heads of all three pigs were beginning to turn black and skin slippage was apparent. The flesh of all three pigs continued to darken and show more slippage throughout the rest of the collection period. The carcasses did not reach the dessication/skeletonization stage of decomposition during this study due to the cold temperatures experienced. The dense GSR deposition and blackening around the gunshot wounds persisted throughout the collection period. The stab wounds in the control pig widened and darkened over time, but stab wounds [Figure 4.8] and gunshot wounds were visually distinguishable throughout this study.

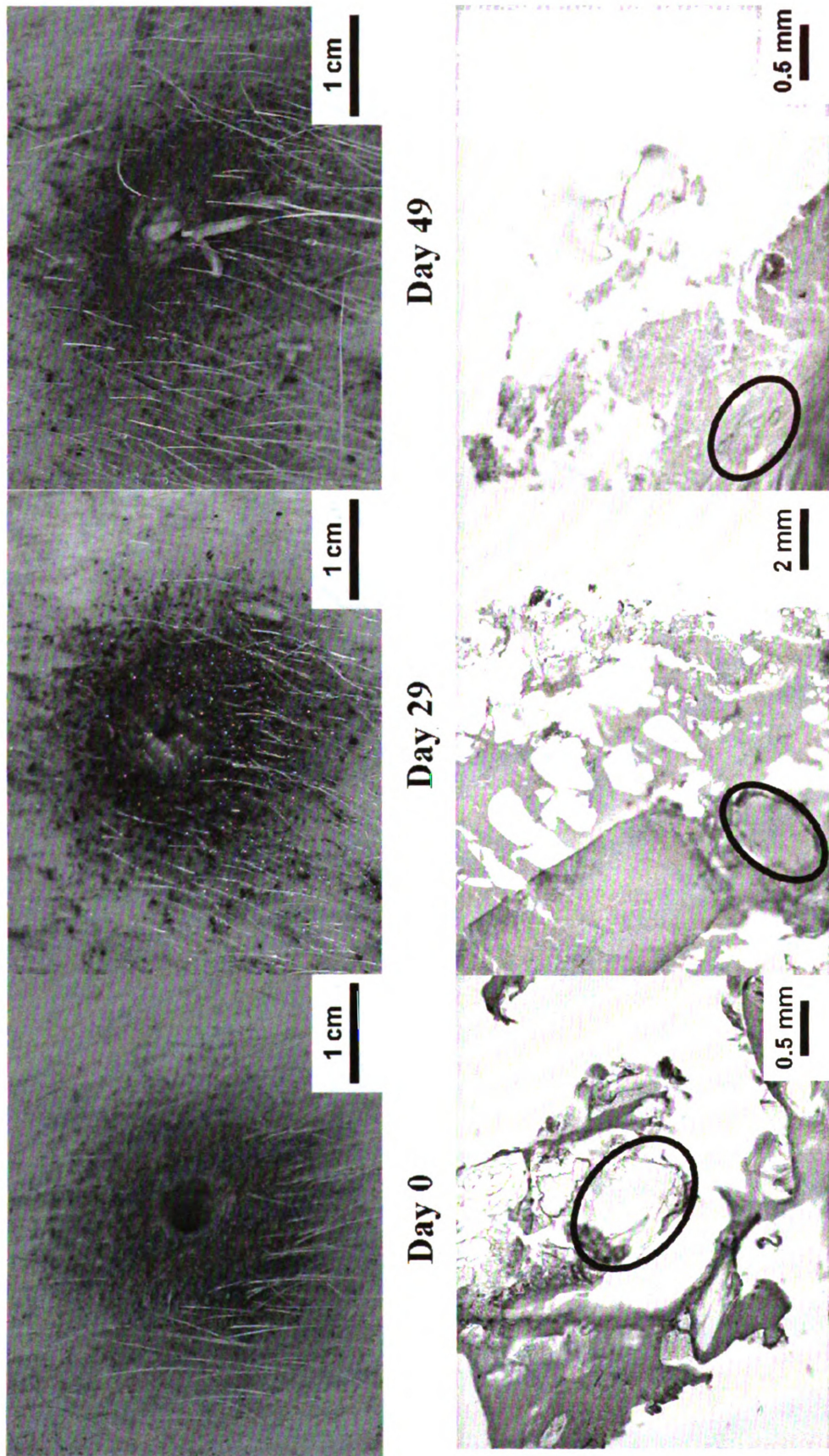


Figure 4.6 – Jacketed bullet wounds on days 0, 29, and 49 during the decomposition study. Corresponding micrographs of H & E stained histology results are shown below the wounds, with particles consistent with GSR circled.



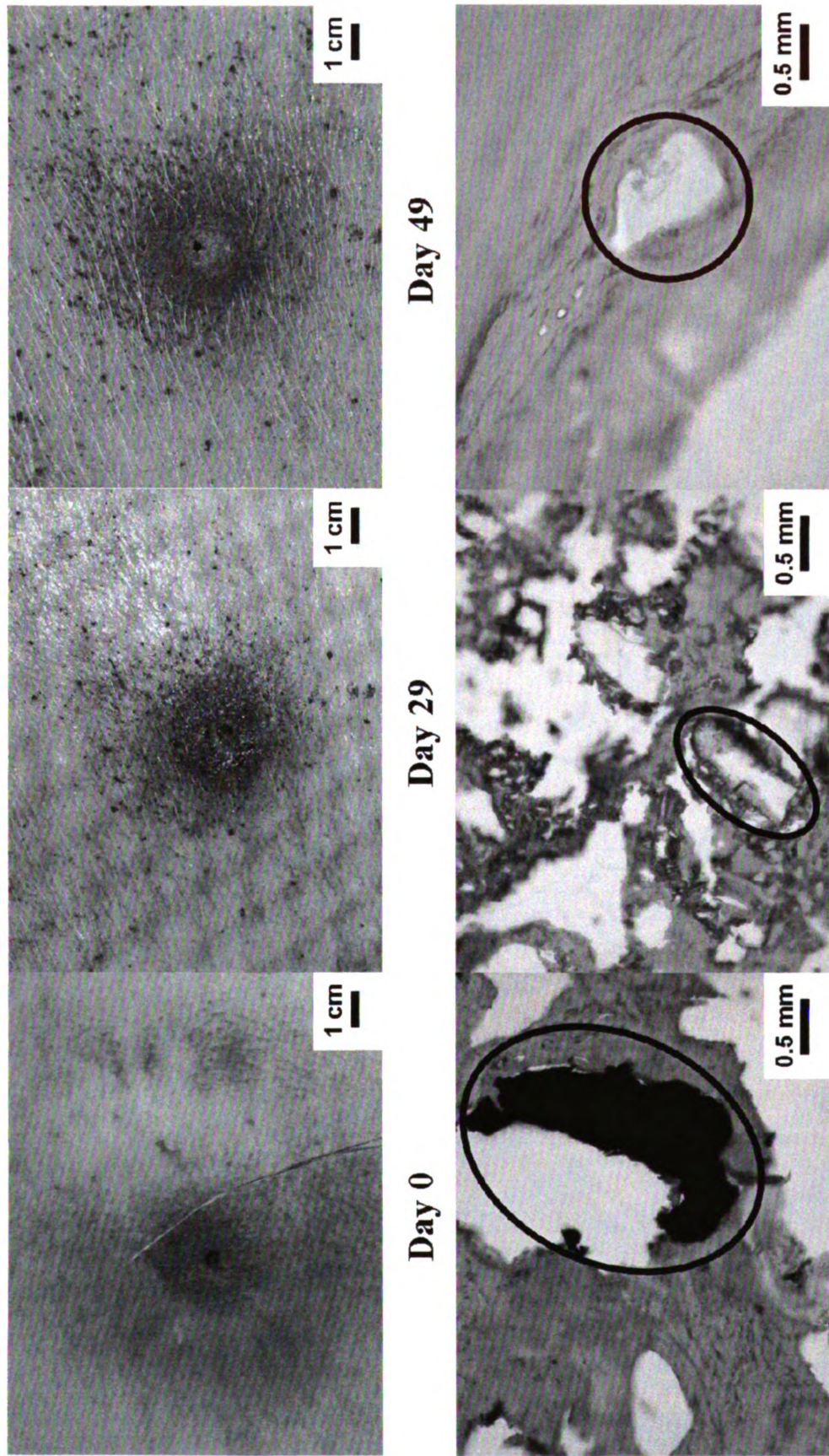


Figure 4.7 – Non-jacketed bullet wounds on days 0, 29, and 49 during the decomposition study. Corresponding micrographs of H & E stained histology results are shown below the wounds, with particles consistent with GSR circled.



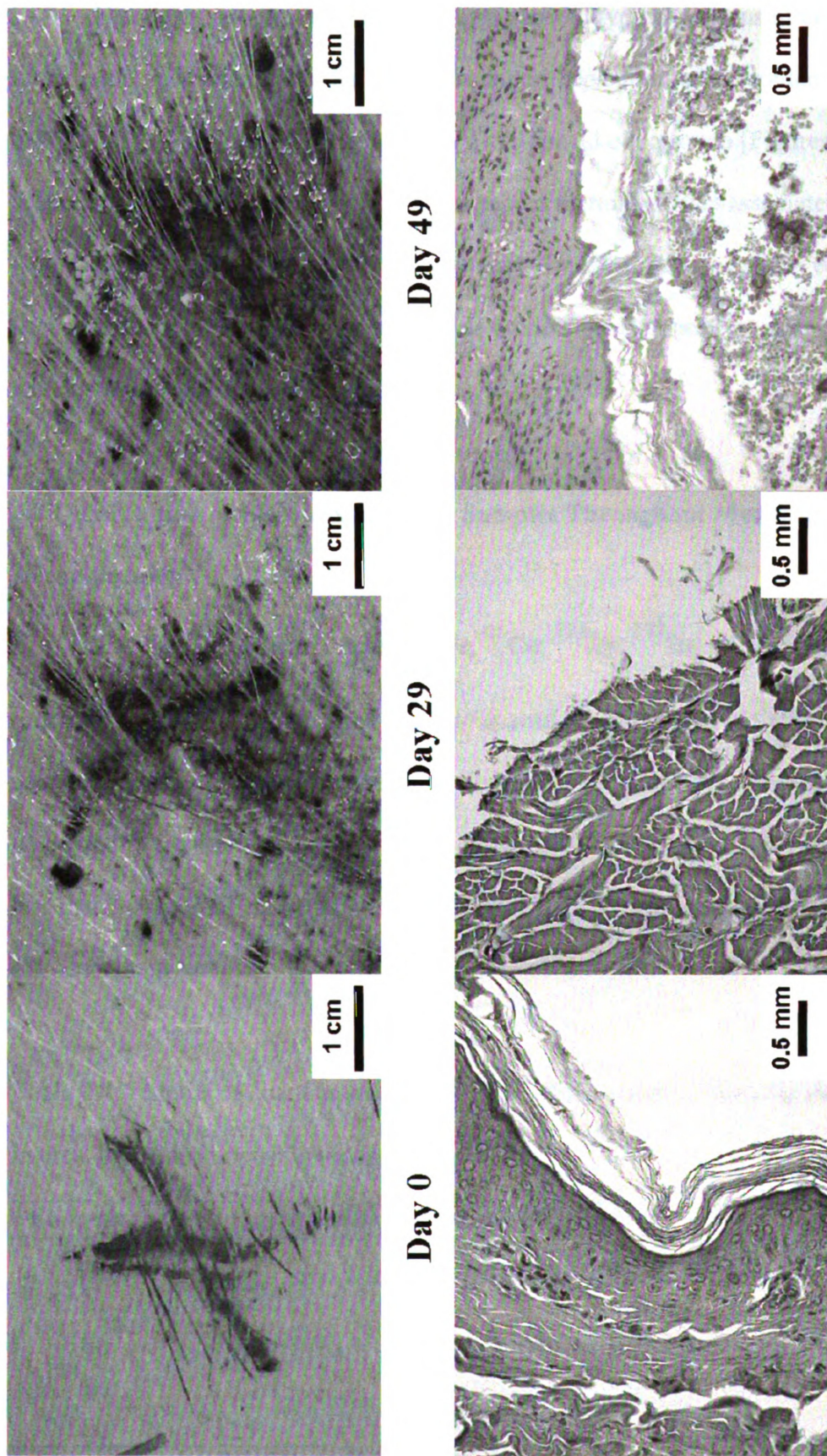


Figure 4.8 – Control (stab) wounds on days 0, 29, and 49 during the decomposition study. Corresponding micrographs of H & E stained histology results did not show any particles consistent with GSR, as expected.

Histology samples from all three pigs showed typical patterns of decomposition, including homogenization of the dermal collagen, separation of the epidermis from the dermis, loss of cellular detail, and bacterial and fungal overgrowth [Figures 4.6-4.8]. The sections at the wound edges showed the expected thermal artifact associated with gunshot wounds, consistent with the fresh tissue studies. The GSR patterns observed in the fresh tissue persisted but decreased in quantity as moderate decomposition progressed in wounds inflicted using both bullet types.

#### **4.8 Quantitation of Elements in Tissue Samples Throughout Moderate Decomposition**

The five elements of interest ( $^{56}\text{Fe}$ ,  $^{63}\text{Cu}$ ,  $^{121}\text{Sb}$ ,  $^{138}\text{Ba}$ , and  $^{208}\text{Pb}$ ) were quantified using ICP-MS, and the limits of quantitation are listed in Table 4.4. The mean concentrations of the five elements in the four SRM samples were calculated and compared to the reported concentrations, as described previously [Table 4.4]. Errors were less than 10% for all elements, indicating the instrument was accurately quantifying the elements in all samples.

Table 4.4 – Limits of quantitation (LOQs) and SRM recovery results for elements of interest in the decomposition study.

<b>Element</b>	<b>LOQ (µg/L)</b>	<b>SRM Average % Error</b>
$^{56}\text{Fe}$	5	0.5
$^{63}\text{Cu}$	5	6
$^{121}\text{Sb}$	< 0.1	4
$^{138}\text{Ba}$	< 0.1	7
$^{208}\text{Pb}$	0.25	5

Since element concentrations were expected to decrease as decomposition progressed, all element signals were monitored in both the undiluted and diluted tissue sample sets. Relatively low levels of  $^{56}\text{Fe}$  and  $^{63}\text{Cu}$  were present throughout the study and hence, these elements were quantitated using the undiluted digest samples so that signals remained within the linear range of the calibration curve. The elements  $^{121}\text{Sb}$ ,  $^{138}\text{Ba}$ , and  $^{208}\text{Pb}$  were more concentrated and were quantitated in the diluted samples to ensure that sample signals remained within the linear calibration curve range and did not saturate the detector.

Concentration ranges for each element of interest throughout moderate decomposition are listed in Table 4.5. The highest element concentrations did not necessarily occur on day 0, and the lowest concentrations did not always correspond to day 49.

Table 4.5 – Element concentration ranges throughout moderate decomposition in each tissue sample type.

<b>Element</b>	<b>Concentration Range (µg/g)</b>		
	<b>Control</b>	<b>Jacketed</b>	<b>Non-Jacketed</b>
$^{56}\text{Fe}$	83-235	348-720	242-438
$^{63}\text{Cu}$	12-27	306-835	99-166
$^{121}\text{Sb}$	10-15	197-3677	1722-3923
$^{138}\text{Ba}$	ND*	1721-18159	5057-16599
$^{208}\text{Pb}$	0-11	702-11010	42753-131245

\* ND indicates “not detected”

Since element concentrations did not appreciably change as decomposition progressed, mean element concentrations were calculated for six tissue samples from each bullet type, collected throughout the study at different stages of decomposition on days 0, 5, 14, 24, 34, and 44 [Figure 4.9]. All elements of interest show higher concentrations in the shot tissue samples relative to the control tissue and procedural blank samples, indicating there was no significant contamination due to the sample preparation method. Mean element concentrations for Cu and Ba (99% confidence level) and for Fe and Pb (95% confidence level) were significantly higher in tissue shot with jacketed ammunition compared to the control tissue. For tissue samples shot with non-jacketed ammunition, all elements were present at significantly higher concentrations in the shot tissue compared to the control tissue at the 99% confidence level. Thus, all elements were suitable for differentiating shot from unshot tissue throughout moderate decomposition.

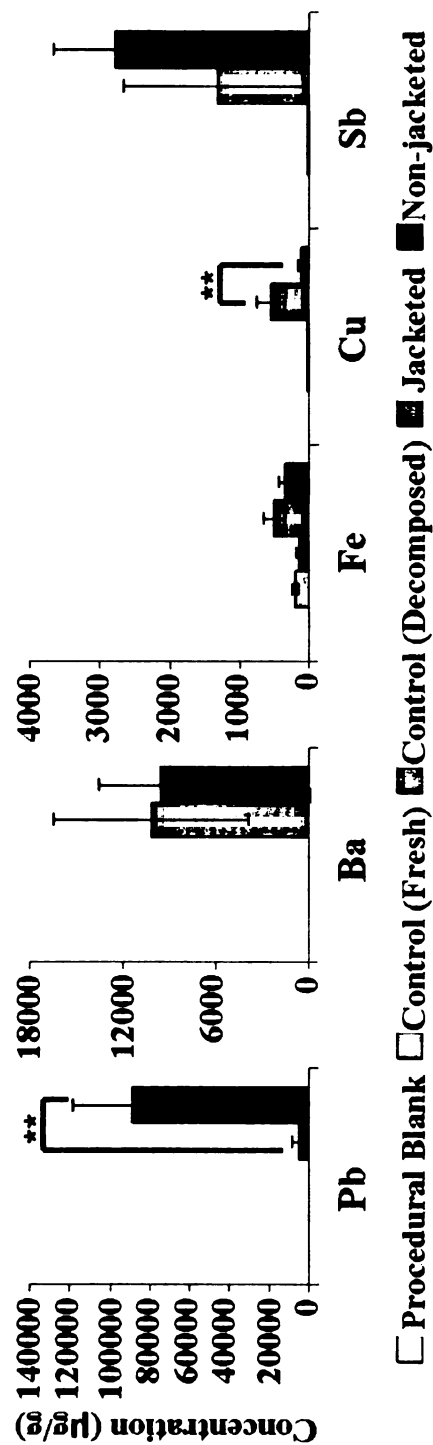


Figure 4.9 – Mean concentrations of elements of interest quantified in samples collected throughout moderate decomposition (procedural blank  $n = 5$ , control (fresh)  $n = 3$ , control (decomposed)  $n = 6$ , jacketed and non-jacketed  $n = 6$ ). The error bars represent one standard deviation. Significant difference between element concentrations at 99% confidence level ( $p \leq 0.01$ ) are indicated by \*\*.



When mean element concentrations were compared between the two bullet types, there were significant differences in the Cu and Pb concentrations at the 99% confidence level [Figure 4.9]. Copper was more concentrated in wounds shot with jacketed bullets, and Pb was more concentrated in tissue shot with non-jacketed bullets, which is likely due to bullet composition, as previously observed in the fresh tissue study. Mean Sb concentrations were not significantly different between the two bullet types in the decomposed tissue samples due to the wide concentration range of this element in the samples shot with jacketed bullets. Some of the variability in element concentrations in GSR was due to the sample collection procedure. Tissue samples for digestion were cut directly adjacent to the entrance wound out to approximately 1 cm, where the GSR was most concentrated. However, as determined in the sampling study, the GSR distribution was not uniform, which leads to differences in element concentrations in the samples, larger standard deviation values, and decreased confidence in element concentration differences between bullet types. Finally, similar to the fresh tissue study, mean Fe and Ba concentrations were not significantly different between the two bullet types and were therefore not useful for differentiation.

Overall, the element concentration results from the decomposed tissue study were similar to results obtained from the fresh tissue study, due to minimal decrease in element concentrations throughout moderate decomposition. All five elements of interest (Fe, Cu, Sb, Ba, and Pb) were able to differentiate shot from unshot tissue, and Cu and Pb were able to discriminate tissue shot with the two different bullet types.

#### 4.9 Principal Components Analysis of Decomposition Study Data

Results from ICP-MS quantitation of the five elements of interest ( $^{56}\text{Fe}$ ,  $^{63}\text{Cu}$ ,  $^{121}\text{Sb}$ ,  $^{138}\text{Ba}$ , and  $^{208}\text{Pb}$ ) in the decomposed tissue samples were further analyzed to examine how element concentrations varied with respect to one another. Principal components analysis (PCA) was used to visualize how different wound samples related to one another overall by comparing the concentrations of the five elements simultaneously, which is more useful than comparing element concentrations individually using Student's *t*-tests as described above. This is also a more objective way to place statistical confidence on the association and discrimination of samples, which is desirable in all forensic analyses. The resulting scores plot is shown in Figure 4.10. Principal component (PC) 1 is the x-axis and accounts for 61% of the variance in the dataset, and PC2 is the y-axis and accounts for 29% of the variance in the samples. Overall, the scores plot shows 90% of the variance in the dataset, meaning that the sample positions are useful approximations of the total chemical variance in the samples projected onto only two dimensions.

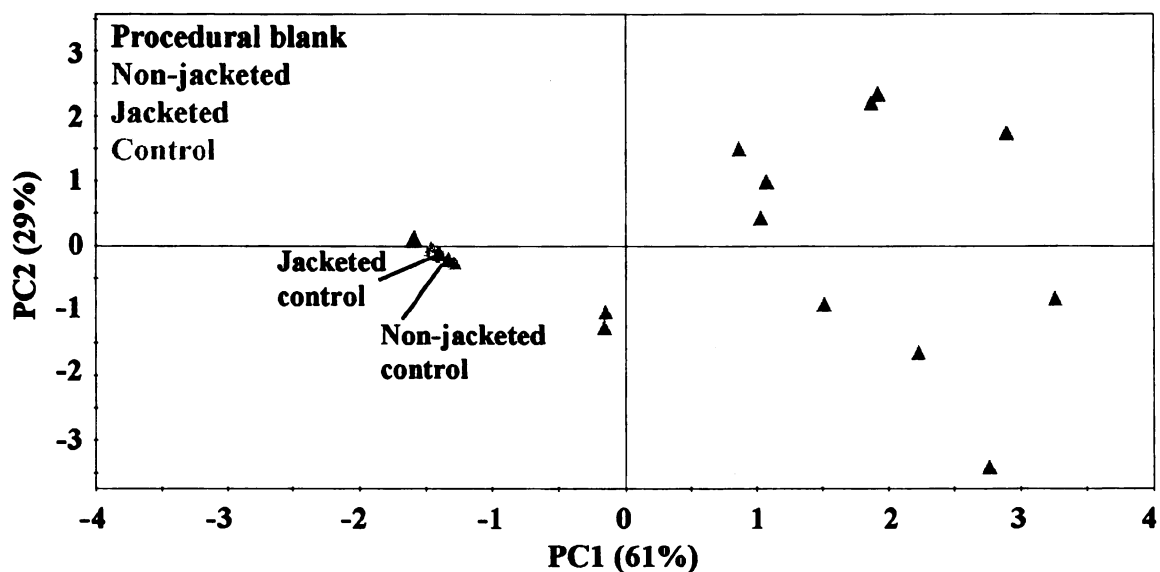


Figure 4.10 – PCA scores plot displaying clustering of chemically similar samples.

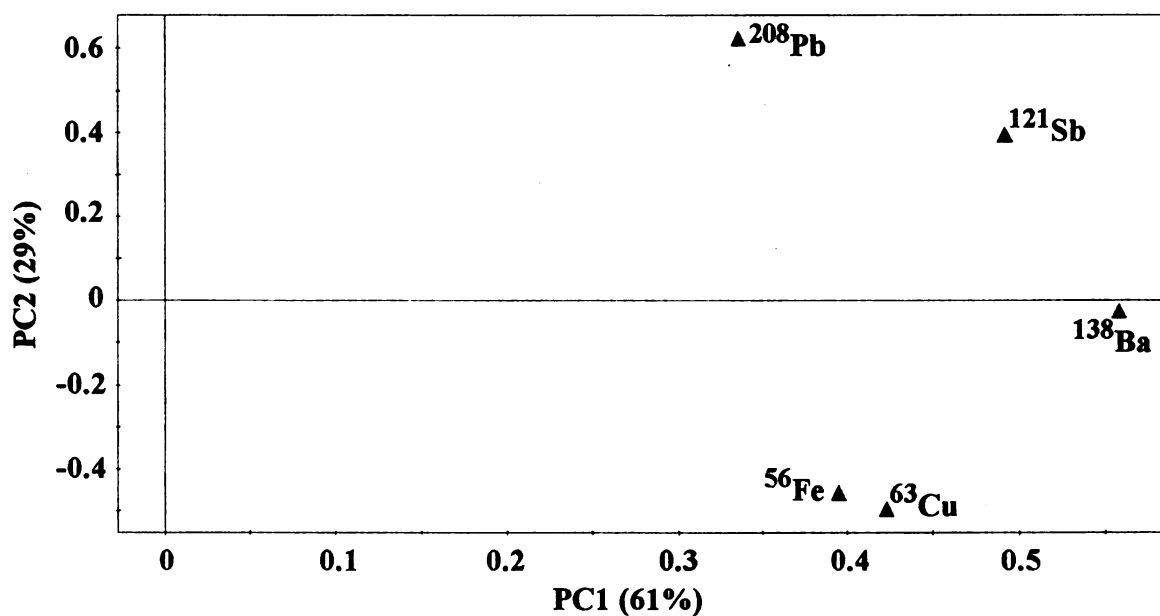


Figure 4.11 – PCA loadings plot showing the elements responsible for the sample positions displayed in the corresponding scores plot.

In the scores plot [Figure 4.10], the procedural blank and control samples group closely, loading negatively on PC1 and near zero on PC2. The five procedural blank samples are overlaid, indicating nearly identical chemical composition as expected for blanks. The control samples taken from the pigs that were subsequently shot with the jacketed and non-jacketed ammunition (labeled “jacketed control” and “non-jacketed control”, respectively) cluster with all of the samples collected from the control (stabbed) pig throughout decomposition, indicating that differences in the shot tissue samples were not simply due to the fact that they were from different pigs. A small amount of spread is observed within the control sample group which is due to natural variability in the tissue samples as they were from different areas of the pig.

All shot tissue samples are positioned more positively on PC1 in the scores plot compared to the procedural blank and control tissue samples. The corresponding PCA loadings plot [Figure 4.11] shows all five elements of interest loading positively on PC1, which corresponds to the positions of the shot tissue samples in the scores plot. This indicates that these five elements are useful for differentiating shot from unshot tissue, supporting the results from the decomposition quantitation study.

The shot tissue samples are separated according to bullet type by PC2 in the scores plot [Figure 4.10], with the samples shot with non-jacketed ammunition positioned positively and the samples shot with jacketed ammunition positioned negatively on PC2. Again, this positioning can be explained with reference to the loadings plot [Figure 4.11]. Lead and Sb load positively on PC2, indicating these two elements correspond to the positions of the samples shot with non-jacketed ammunition on the scores plot. The average Pb concentration in wounds shot with non-jacketed bullets is significantly higher

compared to jacketed bullet wounds, whereas Sb concentrations, though higher in non-jacketed bullet wounds, were not statistically different between the two bullet types in the quantitation study. This explains why Sb is positioned less positively than Pb in the loadings plot. However, the PCA results show that concentrations of both Pb and Sb are systematically higher in wounds shot with non-jacketed bullets compared to wounds shot with jacketed bullets, allowing differentiation of the two bullet types in the scores plot.

All tissue samples shot with jacketed ammunition are positioned negatively on PC2 in the scores plot. Iron and Cu are positioned negatively on PC2 in the loadings plot, indicating that these two elements are associated with the jacketed bullet wound positions on the scores plot. The average Cu concentration was significantly higher in tissue shot with jacketed bullets compared to tissue shot with non-jacketed bullets in the quantitation study, and, though not statistically significant, the average Fe concentration was more abundant in jacketed bullet wounds as well. Thus, the negative positioning on PC2 of the jacketed bullet wounds in the scores plot is due to the higher levels of Cu and Fe in these wounds.

The final element of interest, Ba, is positioned close to zero on PC2, indicating that it is not more closely associated to one group of shot tissue samples than the other. The average Ba concentrations in the jacketed and non-jacketed bullet wounds were nearly identical, indicating that Ba is only useful for differentiating shot from unshot tissue and not for differentiating bullet type.

Therefore, all shot tissue samples are distinct from the procedural blank and control tissue samples, and the tissue samples shot with different ammunition types are clearly separated as well. This indicates considerable chemical composition differences

between the sample groups, which was expected in view of the results from the decomposition quantitation study. There is more spread in the shot tissue samples from both bullet types compared to the tight clustering of the procedural blank and control samples. This is due to variation in element concentration as a result of the effects of moderate decomposition and the random tissue sampling around each wound, as discussed previously.

Overall, PCA results for the five elements of interest in the decomposition study tissue samples were in agreement with observations made from the quantitation study results for Pb, Cu, and Ba. Additionally, Sb and Fe were shown to be useful for differentiating the two bullet types using PCA, despite the lack of statistically significant concentration differences observed during the quantitation study. This is due to the high degree of correlation between the Sb and Pb concentrations and between the Fe and Cu concentrations, which was revealed through PCA. This means that examining all five element concentrations simultaneously allows for more useful tissue sample association and discrimination. Although this is a very small study, it does demonstrate the potential utility of PCA in casework. A questioned tissue sample could be statistically analyzed along with all of these known tissue samples, and the position of the questioned sample on the scores plot could be used to determine whether the questioned wound was a gunshot wound, and if so, whether the questioned gunshot wound was inflicted with either a jacketed or a non-jacketed bullet. However, this is only a proof-of-concept study and considerable further research must be done before this methodology could be implemented in casework.

#### **4.10 References**

1. Stone IC, Di Maio VJM, Petty CS. Gunshot wounds – visual and analytical procedures. J Forensic Sci 1978;23:361-7.
2. Koons RD. Analysis of gunshot primer residue collection swabs by inductively coupled plasma-mass spectrometry. J Forensic Sci 1998;43:748-54.
3. National Oceanic and Atmospheric Administration's National Weather Service. <http://www.weather.gov>.

## CHAPTER 5: CONCLUSIONS AND FUTURE DIRECTIONS

### 5.1 Conclusions

Chemical identification of gunshot residue (GSR) in tissue samples using inductively coupled plasma mass spectrometry (ICP-MS) is a promising option to supplement current gross and histological examination procedures available to coroners, medical examiners, and forensic pathologists. Three studies using ICP-MS for the analysis of fresh gunshot wounds shot with two different ammunition types were completed. The results facilitated selection of an expanded suite of elements capable of differentiating shot from unshot tissue as well as between tissue samples shot with jacketed and non-jacketed bullets. The element distribution in GSR around a non-jacketed bullet wound was also determined in order to develop optimal sampling procedures for this technique. The results from the fresh tissue studies were then applied to decomposed wounds to assess the effects of moderate decomposition on the ability to detect GSR and differentiate bullet types. The ICP-MS results from both fresh and decomposed wounds were compared to corresponding hematoxylin and eosin (H & E) stained histology results to determine if ICP-MS was comparable with the current GSR detection method used by death investigators.

Two fresh wounds, one shot with jacketed ammunition and one shot with non-jacketed ammunition, were analyzed using ICP-MS to detect all elements present. Using several selection criteria, the original suite of elements considered potentially useful for differentiating shot from unshot tissue and differentiating the two bullet types consisted of  $^{24}\text{Mg}$ ,  $^{31}\text{P}$ ,  $^{39}\text{K}$ ,  $^{56}\text{Fe}$ ,  $^{63}\text{Cu}$ ,  $^{66}\text{Zn}$ ,  $^{121}\text{Sb}$ ,  $^{138}\text{Ba}$ , and  $^{208}\text{Pb}$ . Due to instrument limitations, the list of elements of interest was reduced to  $^{56}\text{Fe}$ ,  $^{63}\text{Cu}$ ,  $^{121}\text{Sb}$ ,  $^{138}\text{Ba}$ , and



$^{206}\text{Pb}$ , which showed acceptably low limits of detection, linearity over the calibration range, and accurate concentration determination based on standard reference material recoveries. All five elements of interest were successful in differentiating shot from unshot tissue in the fresh state, and three elements (Cu, Sb, and Pb) were capable of differentiating jacketed and non-jacketed bullet wounds in fresh tissue samples. Antimony and Pb were both more concentrated in tissue shot with non-jacketed bullets (significant at the 99% confidence level), while Cu was more concentrated in tissue shot with jacketed ammunition (significant at the 95% confidence level). The elements that successfully differentiated the bullet types most likely originate from the bullets themselves, since the jacketed bullets have Cu jackets and the non-jacketed bullets are composed of Pb and possibly Sb. Mean Fe and Ba concentrations were not significantly different between the two bullet types, possibly due to these elements originating from the interior of the gun barrel or the ammunition primers, which are more similar in elemental composition between the two ammunition types.

Corresponding results from H & E histology analysis showed particles consistent with GSR in samples from both bullet types. Due to gunpowder composition differences in the two different ammunition types used in this study, the wounds could be distinguished according to bullet type as well. Thus for the fresh tissue studies, the differentiation of shot from unshot tissue as well as tissue shot with two different bullet types could be accomplished using gross examination, histology, and ICP-MS analyses.

The ICP-MS quantitation results from the fresh non-jacketed wound sampling study indicated that the optimal sampling position to detect the five elements considered characteristic of GSR is directly adjacent to the wound and as far out as 2 cm from the

entrance wound in any direction. The high degree of variability in element composition from 2 cm outward prevented detection of some of the characteristic elements and thus did not allow a wound to be definitively identified as a gunshot wound.

These fresh tissue studies allowed the expansion of the suite of elements considered to be characteristic of GSR by adding Fe and Cu to Sb, Ba, and Pb, which are currently considered characteristic of GSR. The addition of these two elements increases confidence in GSR determination, as it is unlikely that these five elements would all be present on a surface due to other materials. Knowledge of the sample position most likely to produce conclusive results for the presence of GSR (adjacent to the entrance wound out to 2 cm) is also vital for coroners, medical examiners, and forensic pathologists.

The optimal sampling procedure was then used to collect tissue samples throughout the decomposition study. The samples were then analyzed by ICP-MS for the suite of characteristic elements present in GSR, and comparisons were made between control tissue samples and samples shot with each bullet type, as well as between the two different bullet types throughout moderate decomposition. Mean element concentrations for Cu and Ba (99% confidence level) and for Fe and Pb (95% confidence level) were significantly higher in tissue shot with jacketed ammunition compared to the control tissue. For tissue samples shot with non-jacketed ammunition, all elements were present at significantly higher concentrations in the shot tissue compared to the control tissue at the 99% confidence level. Thus, all elements were suitable for differentiating shot from unshot tissue throughout moderate decomposition. When mean element concentrations were compared between the two bullet types, there were significant differences in the Cu and Pb concentrations at the 99% confidence level. Copper was more concentrated in

wounds shot with jacketed bullets, and Pb was more concentrated in tissue shot with non-jacketed bullets, which is likely due to bullet composition, as observed in the fresh tissue study.

Corresponding H & E histology results from the decomposition study samples showed particles consistent with GSR throughout moderate decomposition. The different particle patterns from the two different ammunition types persisted but decreased in quantity over the course of the study, and the tissue samples became harder to section and analyze using histology as moderate decomposition progressed.

The ICP-MS results from the decomposed tissue samples were further analyzed using principal components analysis (PCA), which is an objective statistical procedure that was used to examine how all five elements of interest varied with respect to one another in the samples. The results confirmed that all elements were capable of differentiating shot from unshot tissue and that Ba was not able to differentiate the two bullet types. The concentrations of Pb and Sb were determined to be correlated and were higher in non-jacketed bullet wounds. Likewise, the Cu and Fe concentrations were determined to be correlated and were more concentrated in jacketed bullet wounds. These results indicated that these four elements were useful for differentiating tissue shot with the two different bullet types using PCA. Although this was a very small study, it did demonstrate the potential utility of PCA in casework to determine whether a questioned wound was a gunshot wound, and if so, whether the questioned gunshot wound was inflicted with either a jacketed or a non-jacketed bullet. However, this was only a proof-of-concept study, and considerable further research must be done before this methodology could be implemented in casework.

Overall, both histology procedures and ICP-MS were used to identify the presence of GSR in close-range gunshot wounds from two bullet types in both the fresh state and throughout moderate decomposition. However, GSR determination using histology became more difficult as decomposition progressed. Adding the elements Fe and Cu to the elements already considered characteristic of GSR (Sb, Ba, and Pb) increases confidence in gunshot wound determination. Using these element profiles, wounds shot with jacketed bullets were differentiated from wounds shot with non-jacketed bullets throughout moderate decomposition, providing a new level of information to investigators. While this research demonstrated success in differentiating bullet types from close-range gunshot wounds, more challenging tissue samples must be investigated in the future to determine the limitations of these methods.

The results of this research could benefit law enforcement agencies as well as coroners, medical examiners, and forensic pathologists. Law enforcement agencies may use the method to determine the type of bullet used, which can link a weapon and/or suspect to a crime scene. Coroners, medical examiners, and forensic pathologists could use the method to assist in gunshot wound identification and cause of death determination, even in corpses in a moderate state of decomposition.

## **5.2 Future Directions**

Now that the capability to differentiate close-range jacketed and non-jacketed bullet wounds using ICP-MS has been established, there are numerous possibilities for future studies. As all studies using ICP-MS for GSR detection have been conducted using close-range wounds, it would be useful to examine the capabilities and limitations of

ICP-MS for GSR determination in wounds shot from farther distances. Tissue samples shot from known distances and analyzed using ICP-MS to quantitate the elements of interest identified in this study may provide a relationship between the concentration of certain elements and firing distance. Depending on the results of the initial study with one bullet type, the differentiation of multiple bullet types at farther distances could also be investigated. If that were successful, then the potential to determine firing distance and bullet type throughout the course of decomposition could be tested in a similar manner. Any information from successful outcomes of these experiments would be considered very useful to law enforcement officers and death investigators.

The current studies investigated only one gun and the two most common bullet types, but there are many others types of firearms and ammunition readily available. Carrying out studies comparing the GSR detected by ICP-MS from different common firearms, such as semi-automatics and even rifles and shotguns, as well as their associated ammunition types would add to the knowledge base in this area of forensics. Also, only one ammunition manufacturer was investigated in the present study. It would be interesting to examine how elemental compositions vary for the same ammunition type obtained from different manufacturers. Ideally, elemental profiles of the same type of ammunition from different manufacturers would be similar enough to differentiate between bullet types from several different manufacturers. In addition, there was a difference in the type and amount of gunpowder in the two different ammunition types from the same manufacturer used in these studies. It would be interesting to investigate differentiation of ammunition with the same gunpowder and different bullet types both using histology and ICP-MS for GSR detection.

All tissue samples that have been analyzed for the presence of GSR using ICP-MS have been relatively free of environmental debris and have decomposed above ground. The case that provided the idea for this research involved a body that was buried for a year before discovery and autopsy. Studies simulating the conditions of this case need to be conducted in order to address the challenges of gunshot wound determination routinely seen in casework. Pigs could be shot and then buried throughout the decomposition process, and the wounds would be analyzed by ICP-MS to determine if the soil interfered with GSR element detection. Burying the pigs at different depths and in different soil types in different seasons of the year would also be essential, as the decomposition process is affected by all of these parameters. The ability to differentiate ammunition types and possibly also gain information about the range of fire from buried tissue samples could also be explored if preliminary studies were successful.

Finally, as hematoxylin and eosin (H & E) staining of histology samples is not designed to enhance visualization of GSR particles, staining tissue sections with different reagents that are designed to indicate the presence of elements contained in GSR would be useful. Stains are available that react with the currently accepted GSR elements (Ba and Pb), and evaluating their ability to determine the presence of GSR in wounds in both the fresh state and throughout decomposition in comparison to ICP-MS would be useful for coroners, medical examiners, and forensic pathologists. If successful, the stains could be used on more challenging tissue samples, such as those shot from farther distances, shot with different ammunition types, and buried in the ground. Samples could also be analyzed by ICP-MS as a comparison to determine the most useful technique for GSR determination in decomposed tissue samples.

## APPENDIX

Weather data from the decomposition study sample collection period.

Day	Date	Temperature (°F)			Rain (in.)	Samples Taken
		Maximum	Minimum	Average		
0	10/2/2009	57	48	53	0.39	X
1	10/3/2009	57	47	52	0.08	
2	10/4/2009	58	48	53	0.01	X
3	10/5/2009	59	44	52	-	
4	10/6/2009	61	42	52	0.20	
5	10/7/2009	57	42	50	trace	X
6	10/8/2009	60	41	51	0.06	
7	10/9/2009	51	44	48	0.56	
8	10/10/2009	53	32	43	-	
9	10/11/2009	47	27	37	-	X
10	10/12/2009	49	34	42	0.01	
11	10/13/2009	49	32	41	0.01	
12	10/14/2009	46	31	39	trace	
13	10/15/2009	45	37	41	trace	
14	10/16/2009	45	33	39	-	X
15	10/17/2009	49	27	38	-	
16	10/18/2009	50	26	38	-	
17	10/19/2009	62	38	50	-	
18	10/20/2009	61	47	54	-	
19	10/21/2009	69	52	61	0.17	X
20	10/22/2009	58	41	50	0.32	
21	10/23/2009	59	41	50	0.99	
22	10/24/2009	50	39	45	0.03	
23	10/25/2009	58	37	48	trace	
24	10/26/2009	64	48	56	0.01	X
25	10/27/2009	56	47	52	0.08	
26	10/28/2009	54	41	48	0.02	
27	10/29/2009	59	39	49	trace	
28	10/30/2009	69	51	60	1.11	
29	10/31/2009	54	40	47	trace	X
30	11/1/2009	49	35	42	-	
31	11/2/2009	52	38	45	0.08	
32	11/3/2009	46	31	39	-	
33	11/4/2009	48	29	39	trace	
34	11/5/2009	49	28	39	trace	X

35	11/6/2009	49	25	37	-	
36	11/7/2009	67	44	56	-	
37	11/8/2009	70	35	53	-	
38	11/9/2009	67	49	58	-	
39	11/10/2009	54	36	45	-	X
40	11/11/2009	53	28	41	-	
41	11/12/2009	52	22	37	-	
42	11/13/2009	59	29	44	-	
43	11/14/2009	64	43	54	-	
44	11/15/2009	59	40	50	trace	X
45	11/16/2009	48	38	43	-	
46	11/17/2009	50	33	42	-	
47	11/18/2009	56	35	46	0.16	
48	11/19/2009	48	41	45	0.25	
49	11/20/2009	48	42	45	0.01	X

---



MICHIGAN STATE UNIVERSITY LIBRARIES



3 1293 03063 7817